Vapor and Liquid (p-ρ-T-x) Measurements of Binary Refrigerant Blends Containing R-32, R-152a, R-227ea, R-1234yf, and R-1234ze(E)*

Tara J. Fortin†
Mark O. McLinden

National Institute of Standards and Technology
Material Measurement Laboratory
Applied Chemicals and Materials Division
325 Broadway
Boulder, CO 80305-3328, U.S.A.

Phone: 1-303-497-3522
Fax: 1-303-497-6682
E-Mail: tara.fortin@nist.gov

† Corresponding author.

Abstract

The pressure-density-temperature-composition (p-ρ-T-x) data of binary refrigerant mixtures containing R-32 (difluoromethane), R-152a (1,1-difluoroethane), R-227ea (1,1,1,2,3,3,3-heptafluoropropane), R-1234yf (2,3,3,3-tetrafluoropropene), and R-1234ze(E) (*trans*-1,3,3,3-tetrafluoropropene) were measured in both the vapor and liquid phases using a two-sinker, magnetic-suspension densimeter. The specific samples in this study comprised two compositions of approximately (0.3/0.7) molar and (0.7/0.3) molar for each of the following four binary refrigerant blends: R-32 + R-1234yf, R-32 + R-1234ze(E), R-1234yf + R-152a, and R-1234ze(E) + R-227ea. Single-phase vapor densities were measured over a temperature range of approximately (253 to 293) K and pressures from (0.05 to 0.98) MPa. Single-phase liquid and supercritical densities were measured over a temperature range of approximately (230 to 400) K and pressures up to 22 MPa; for refrigerant blends containing R-1234yf the maximum pressure was limited to 14 MPa. Overall relative combined, expanded ($k = 2$) uncertainties in density ranged from 0.025% to 0.191%, with an average uncertainty of approximately 0.05%. Here we present measurement results, along with comparisons to available literature data and to default equations of state and mixture models included in REFPROP.

Keywords

Density; hydrofluorocarbons; hydrofluoroolefins; refrigerant blends

1. Introduction

In 1987, in response to scientific evidence linking anthropogenic emissions of ozone-depleting chlorofluorocarbons (CFCs) to the observed thinning of the ozone layer over Antarctica, the United Nations adopted the Montreal Protocol which established a framework for the global phase-out of the production and consumption of ozone-depleting substances.[1] The agreement went into effect on January 1, 1989, and has since undergone several revisions.[2] Consequently, hydrofluorocarbons (HFCs) have replaced CFCs in a broad range of applications and equipment including air conditioners, domestic and medium-temperature refrigeration systems, aerosol propellants, and foam blowing agents.[3]

Because HFCs do not contain chlorine, they pose no harm to the ozone layer, but they have been identified as potent greenhouse gases (GHGs). The global warming potential (GWP) facilitates comparisons of the climate impacts of different gases by providing a measure of the amount of heat trapped by 1 ton of gas over a specified period of time (e.g., 100 years) relative to 1 ton of carbon dioxide.[4] For example, HFC R-134a, which was the primary replacement for R-12, has a GWP_{100} of 1530.[5, 6] As a result, more recent measures have targeted HFCs for production and emissions reductions. In 1997, the Kyoto Protocol to the United Nations Framework Convention on Climate Change committed signatories to targeted reductions in GHG emissions, including HFCs.[7] In 2006, the European Union fluorochemical (or "F-Gas") regulations mandated that the GWP_{100} of refrigerants used in automotive air conditioners not exceed 150.[8, 9] In 2014, updated regulations mandated maximum GWP values for refrigerants in additional applications throughout the European Union.[10] In the United States, the Environmental Protection Agency's (EPA) Significant New Alternatives (SNAP) program specifies acceptable and unacceptable refrigerants for each major industrial use sector.[11] In 2016, the Kigali Amendment to the Montreal

Protocol called for an eventual reduction in the GWP-weighted production of HFCs by 80-85%, depending on the country.[12]

These recent regulatory efforts have sparked the development of the next generation of refrigerants with zero ozone depletion potential (ODP) and low GWP. Extensive analyses of potential low GWP refrigerants have demonstrated that only a limited group of fluids exhibit the properties required for low- and medium-temperature refrigeration applications.[13-16] Of this limited set of candidates, hydrofluoroolefins (HFOs) are considered one of the most promising groups of compounds. Similar to HFCs, the lack of chlorine makes HFOs safe for the ozone layer. But unlike HFCs, the presence of a double bond makes HFOs highly reactive with hydroxyl radicals (OH) in the atmosphere resulting in lifetimes of days to weeks compared to lifetimes of years to decades for most HFCs. This translates to very low GWPs. For example, the two HFOs included in this study, R-1234yf and R-1234ze(E), have an estimated GWP_{100} of < 1 and 1, respectively.[17]

R-1234yf (2,3,3,3-tetrafluoropropene) was developed as a replacement for R-134a in mobile air conditioners and has been adopted by many automobile manufacturers despite the fact that its volumetric cooling capacity has been demonstrated to be lower than that of R-134a under some operating conditions.[18-20] Similar limitations were observed with pure R-1234ze(E) (*trans*-1,3,3,3-tetrafluoropropene) during an investigation of its viability as a drop-in replacement for R-410A (a 50/50 mass % mixture of R-32 and R-125) in domestic heat pump systems.[21] Additionally, both R-1234yf and R-1234ze(E) are mildly flammable with an A2L safety classification under ANSI/ASHRAE Standard 34.[22] In an effort to overcome performance limitations of individual pure-fluid refrigerants such as those highlighted above, the refrigeration community is actively investigating blends of HFOs with more traditional refrigerants.

The measurements presented here were part of a larger project aimed at identifying new energy efficient refrigerants that could be adopted by the heating, ventilation, and air conditioning (HVAC) industry. Such a shift is required if the U.S. is to meet its obligations under the Kigali Amendment. The development of accurate models to effectively analyze the performance of candidate blends in HVAC applications requires reliable thermophysical property data. In this work, we report pressure-density-temperature-composition (p-ρ-T-x) measurements in the single-phase and supercritical regions for four binary refrigerant blends: R-32 + R-1234yf, R-32 + R-1234ze(E), R-1234yf + R-152a, and R-1234ze(E) + R-227ea. Overall, these measurements covered temperatures from approximately (230 to 400) K and pressures up to 22 MPa, and for each blend sample compositions were approximately (0.3/0.7) molar and (0.7/0.3) molar. The measurements presented here are part of a larger project, the scope of which included comprehensive measurements of vapor-liquid equilibria (VLE) and speed of sound.[23-26] These measurement results have been used to develop new mixture models, which are published separately.[27, 28] The new models will ultimately replace existing models in REFPROP (Version 10.0), which are presently based upon estimation schemes or unpublished models in many cases.[29, 30]

2. Materials and Methods

2.1 Refrigerant Blends

The five refrigerants used in the blends studied in this work are listed in Table 1 along with corresponding chemical formula, CAS number, supplier, and supplier's stated purity. Molecular diagrams for each of the refrigerants are shown in Figure 1. All five refrigerants have stated purities

of 99.9% or higher; this was verified via gas chromatography-mass spectrometry (GC-MS) analyses performed at NIST which found no significant impurities.

In addition to the two HFOs R-1234yf and R-1234ze(E) previously discussed, the blends studied in this work include three HFCs: R-32 (difluoromethane), R-152a (1,1-difluoroethane), and R-227ea (1,1,1,2,3,3,3-heptafluoropropane). Its superior thermodynamic properties has led R-32 to be used as a replacement for R-22 and R-410A in residential air conditioners;[31, 32] however it has a moderately high GWP_{100} of 771[5, 6] and is mildly flammable with an A2L safety classification under ANSI/ASHRAE Standard 34.[22] R-152a is commonly used as an aerosol propellant and foam-blowing agent and is considered a potential replacement for R-134a in domestic refrigerators;[33] it has a lower GWP than R-32 (GWP_{100} = 164)[5, 6] but is more flammable with an A2 safety classification.[22] Finally, R-227ea is used as a fire suppression agent and aerosol propellant; unlike the other two HFCs used in this study, it is not flammable with an A1 safety classification,[22] but it has an extremely high GWP_{100} of 3600.[5, 6] Nevertheless, it is of interest as a blend component because of its ability to suppress flammability.

Prior to preparing the mixtures, each individual fluid was transferred to stainless steel sample cylinders and degassed by freezing the pure components in liquid nitrogen, evacuating the vapor space over the frozen sample, then thawing the sample; this freeze-pump-thaw cycle was repeated until the residual pressure over the frozen sample was < 0.01 Pa. Additional details of the degassing procedure can be found in Outcalt and Rowane.[23]

The gas-phase mixtures were prepared gravimetrically in aluminum sample cylinders with approximate internal volumes of 6, 10 or 13 L depending on the pressure of a given mixture. Specifically, the sample cylinders were loaded to pressures below the dew-point pressure at T = 293.15 K; despite this, it is possible that a small amount of liquid was present in the sample

cylinders after filling. Therefore, the cylinders were heated continuously to $T > 313$ K to ensure that only single-phase vapor was present during testing. The sample mass was determined via a double substitution weighing scheme[34] with a nearly identical "tare" or reference cylinder serving as the main substitution mass. This approach minimizes potential errors associated with a non-linear balance response and air buoyancy effects. Additional details regarding the procedure used during the gravimetric preparation of the refrigerant mixtures can be found in Richter and McLinden.[35] The final compositions for each of the eight measured samples are reported in Table 2, along with the total sample volume. It should be noted that the 6 L and 10 L samples were prepared using a balance with a 10 kg maximum capacity and a 0.1 mg resolution, while the 13.4 L samples utilized a balance with a 41 kg maximum capacity and a 1 mg resolution.

The standard uncertainty in the composition due to the gravimetric preparation alone was estimated to be approximately 0.00005 mole fraction. Additional sources of uncertainty include sample purity, contamination of the outside of the cylinder, cylinder expansion upon filling, sorption effects as described in detail by Richter and McLinden,[35] and uncertainties associated with loading of the sample into the densimeter. These additional uncertainty contributions are discussed in greater detail in Section 3.2.

2.2 Apparatus Description

The measurements reported here utilized a two-sinker densimeter, which provides an absolute determination of density via application of the Archimedes, or buoyancy, principle. The use of two sinkers improves the accuracy of the technique as described by Kleinrahm and Wagner[36] and Wagner and Kleinrahm.[37] The densimeter used in this work has previously been described in detail by McLinden and Lösch-Will[38] so only a brief description is provided here.

Two sinkers with nearly identical masses and surface areas, but drastically different volumes, were separately weighed with a high-precision balance while immersed in a fluid of unknown density. The fluid density, ρ, is given by

$$\rho = \frac{(m_1 - m_2) - (W_1 - W_2)}{(V_1 - V_2)}, \quad (1)$$

where m is the sinker mass, V is the sinker volume, W is the balance reading, and the subscripts refer to the two sinkers. In this work, one sinker was made of tantalum with m = 60.094633 g and V = 3.60872 cm^3, while the other sinker was made of titanium with m = 60.075386 g and V = 13.315284 cm^3. A magnetic suspension coupling transmitted the gravity and buoyancy forces on the sinkers to the balance, thus isolating the fluid sample from the balance. The main advantage of a two-sinker densimeter is that the systematic errors in the weighing and from other sources approximately cancel, resulting in greater accuracy relative to other buoyancy techniques.

For each density determination, two calibration masses (referred to as "cal" and "tare") were also weighed by placing them directly on the balance pan; doing so calibrated the balance and provided information needed to correct for magnetic effects as described by McLinden et al.[39] and Kleinrahm et al.[40] The two sinker weighings and two calibration mass weighings yielded a set of four equations that were solved to produce a balance calibration factor, α, and a parameter describing the efficiency of the magnetic suspension coupling, ϕ. The fluid density could then be calculated as

$$\rho = \left\{\left[(m_1 - m_2) - \frac{(W_1 - W_2)}{\alpha\phi}\right]/(V_1 - V_2)\right\} - \rho_0, \quad (2)$$

where ρ_0 is the indicated density when the sinkers are weighed in vacuum, and it accounts for small changes in sinker masses with time. Density as calculated with eq 2 compensates for the magnetic effects of both the apparatus and the fluid being measured; the magnitude of the force transmission error is indicated by the difference of the value of ϕ from 1.[39, 40] In this work ϕ varied

from 1.000003 to 1.000004 in vacuum and from 0.999950 to 1.000048 during refrigerant blend measurements.

The densimeter was thermostated with a multi-layer, vacuum-insulated thermostat. The measuring cell was surrounded by a copper shield with heaters at the top and side; this "inner shield" was surrounded by an additional isothermal shield with heaters at the top and sides and a fluid cooling channel at the top. This second "outer shield" was maintained at a temperature approximately 1 K below that of the measuring cell. A chiller circulating ethanol through the fluid channel on the outer shield was used for measurements at subambient temperatures.

The temperature inside the measuring cell was measured with a 25 Ω standard platinum resistance thermometer (SPRT) and an AC resistance bridge referenced to a thermostated standard resistor. In this work, the cell temperature was constant to within 5 mK. Pressures were measured using one of three vibrating-quartz-crystal type pressure transducers with full-scale pressure ranges of 2.8 MPa, 13.8 MPa, or 68.9 MPa. All three transducers, as well as the pressure manifold, were thermostated at $T = (313.15 \pm 0.20)$ K to minimize the effects of laboratory temperature variations.

2.3 Experimental Procedures

Vapor-phase densities were measured along isotherms at approximate temperatures of 253.15 K, 263.15 K, 273.15 K, 283.15 K, and 293.15 K. For each isotherm, approximately (49 to 146) kPa of fresh sample was introduced into the evacuated measuring cell; the pressure was subsequently increased in steps by cycling two pneumatic valves piped in series. At each new pressure, four replicate density determinations were made following an initial equilibration period of 30–60 min.

Liquid and supercritical phase densities were determined from a combination of measurements along isochores and isotherms carried out over temperatures from approximately

(230 to 400) K. To load liquid sample, the evacuated measuring cell was cooled and gas-phase sample from the sample bottle was then condensed into the cell (see Section S1 of Supporting Information for additional information regarding sample loading). Higher pressures were obtained by closing the valve between the sample manifold and the measuring cell and increasing the cell temperature in steps along a pseudoisochore. It should be noted that the maximum pressure was limited to 14 MPa for refrigerant blends containing R-1234yf to avoid potential polymerization reactions.[41] As with the vapor-phase measurements, once a new setpoint temperature and pressure was reached, an additional equilibration time of 30–60 min was allowed, after which four replicate density determinations were carried out. When the maximum desired pressure along a pseudoisochore was reached, the pressure was decreased by venting a portion of the sample into a waste bottle. Measurements were made in this manner along an isotherm to a minimum pressure of approximately 1 MPa or slightly above the bubble-point pressure, whichever was higher. Measurements were then resumed at increasing temperatures along the next, lower-density pseudoisochore. Following this procedure allowed us to avoid possible contamination from the use of a pump or compressor and minimized the number of manual sample-handling steps.

The measurement cell and all filling/pressure lines were evacuated for a minimum of 36 h between each measured blend composition, as well as before and after all testing. This was done to ensure the complete removal of the previously measured sample and to check the zero of the pressure transducers and the ρ_0 of the apparatus (eq 2). In this work, the ρ_0 varied by less than 0.0010 kg·m^{-3}. Additionally, for each blend composition, vapor measurements were completed before moving on to the liquid and supercritical measurements and the cell and all lines were purged a minimum of three times prior to filling for the first vapor isotherm.

3. Results and Discussion

3.1 Measurement Results

The measured (p-ρ-T-x) state points for the eight samples studied in this work are shown in Figures 2 and 3, plotted as density vs temperature; data for the blends containing R-1234yf are shown in Figure 2, while those for the blends containing R-1234ze(E) are shown in Figure 3. More specifically, for the R-32 + R-1234yf blends, results for the x_1 = 0.33681 molar sample are shown in Figure 2a, and results for the x_1 = 0.67205 molar sample are shown in Figure 2b. For R-1234yf + R-152a, results for the x_1 = 0.33342 molar sample are shown in Figure 2c, while those for the x_1 = 0.66526 molar sample are shown in Figure 2d. Similarly, for the R-32 + R-1234ze(E) blends, results for the x_1 = 0.33512 molar sample are shown in Figure 3a, and results for the x_1 = 0.66665 molar sample are shown in Figure 3b. For the R-1234ze(E) + R-227ea blends, results for the x_1 = 0.33265 molar sample and the x_1 = 0.66803 molar sample are shown in Figures 3c and 3d, respectively. For all eight samples, all replicate density determinations are shown, and the experimental temperatures are averages of readings taken over the 12 minutes needed to complete a single density determination. It should be noted that the data shown in Figures 2 and 3 are also presented in Tables S1–S8 of the Supporting Information for reference. Also shown in Figures 2 and 3 are the corresponding phase boundaries (red line) and the critical points (red asterisk) calculated using REFPROP.[30] Points below the phase boundary line are vapor-phase measurements, while those above and to the right are liquid and supercritical phase measurements.

The measured data for the eight refrigerant blend samples are also presented in Tables 3–10; in contrast to the data shown in Figures 3 and 4, these data are averages of the replicate measurements made at each (T, p) state point. Also included in Tables 3–10 are the associated standard uncertainty in pressure ($u(p)$) and the relative combined, expanded (k = 2) state-point uncertainty in density ($100\cdot(U(\rho)/\rho)$). Details regarding the uncertainty analysis are discussed in

Section 3.2. Finally, Tables 3–10 include relative deviations from the default models contained in REFPROP (Version 10.0)[30] ($\Delta\rho$) which were calculated as

$$\Delta_\rho = 100 \cdot \left(\frac{\rho_{\mathrm{exp}} - \rho_{\mathrm{REF}}}{\rho_{\mathrm{REF}}}\right), \tag{3}$$

where ρ_{exp} is the experimentally determined density and ρ_{REF} is the density calculated using REFPROP.[30] The observed deviations relative to REFPROP[30] will be discussed in detail in Section 3.3.

3.2 Measurement Uncertainty

A detailed analysis of the measurement uncertainty associated with density data collected with the two-sinker densimeter has been reported in previous works;[38, 42, 43] only a brief discussion is given here. The main sources of uncertainty in density, in order of significance, were the sinker volumes (V_1, V_2), the weighings of the sinkers and calibration masses (W_1, W_2, W_{cal}, W_{tare}), the masses of the sinkers and calibration masses (m_1, m_2, m_{cal}, m_{tare}), and the apparatus zero ρ_0. Also included, was the variance in the replicate balance readings. The standard uncertainty in the density measurement is given by

$$u(\rho) = 10^{-6}\rho \cdot \sqrt{\{28\}^2 + \{0.38(T - 293)\}^2 + \{0.63p\}^2} + 0.0010, \tag{4}$$

where the radical term represents the uncertainty in the sinker volumes and the final, constant term incorporates all other uncertainties. In eq 4, $u(\rho)$ and ρ are in units of kg·m^{-3}, T is in K, and p is in MPa. The standard uncertainty in density as expressed by eq 4 does not take into consideration the effects of temperature, pressure, or mixture composition. These additional contributions are discussed next.

The SPRT used to measure the temperature was calibrated on ITS-90 from 234 K to 505 K using multiple fixed-point cells. The estimated standard uncertainty in temperature was 3 mK; this

included the uncertainty in the fixed point cells, drift in both the SPRT and the standard resistor, and any temperature gradients. The three pressure transducers were calibrated with gas-operated piston gages. The standard uncertainty in pressure included the uncertainty in the pressure transducers, as well hydrostatic head correction effects; it was estimated to be ($20\times10^{-6}\cdot p$ + 0.03 kPa) for the vapor-phase measurements and ($26\times10^{-6}\cdot p$ + 1.0 kPa) for the liquid-phase measurements. Additionally, the observed standard deviations in measured temperature, pressure and balance readings made over a complete 12 minute density determination were added to the above uncertainty estimates.

Finally, for mixtures, uncertainty in the composition contributes significantly to the overall uncertainty in density. The uncertainty analysis presented here follows the example discussed in detail by Richter and McLinden.[35] As was previously mentioned, the uncertainty in composition arises, in part, from the gravimetric preparation of the gas mixture, but possible adsorption of sample onto the inner walls of the sample cylinder, filling lines, measuring cell, etc. contributes more significantly. The uncertainty from adsorption effects was estimated to contribute approximately 0.0052 $g\cdot mol^{-1}$.[35] Additionally, the uncertainty in sample purity was estimated to contribute approximately ($0.0002\cdot\rho$) $kg\cdot m^{-3}$. Consequently, including all additional sources of uncertainty, the absolute combined, standard uncertainty in density resulting from the uncertainty in composition was estimated to be (0.0003–0.2783) $kg\cdot m^{-3}$ (see the accompanying Supporting Information).

When comparing (p, ρ, T, x) measurements to a model, it is common to assume that the temperature, pressure, and composition are known exactly, and to combine all uncertainties into a single so-called expanded ($k = 2$) state-point uncertainty for density using the following expression

$$U(\rho) = 2 \cdot \sqrt{[u(\rho)]^2 + \left[\left(\frac{\partial \rho}{\partial p}\right)_T u(p)\right]^2 + \left[\left(\frac{\partial \rho}{\partial T}\right)_p u(T)\right]^2 + \left[u_\rho(x)\right]^2} \quad , \tag{5}$$

where the radical terms represent the standard uncertainties in density (calculated via eq 4), pressure, temperature, and composition, all expressed in units of $kg \cdot m^{-3}$. The uncertainties calculated using eq 5 were used to derive the relative combined, expanded state-point uncertainties reported in Tables 3–10. Overall, the observed uncertainties ranged from 0.025% to 0.191%, with an average uncertainty of approximately 0.05%. In general, the largest relative uncertainties were associated with vapor-phase measurements.

3.3 Data Comparisons

The comprehensive thermophysical property measurement results from this project have been used to improve upon existing mixture models. The mixture models included in REFPROP[30] utilize pure component Helmholtz energy empirical multi-parameter equations of state (EoS), combined with binary interaction parameters and mixing rules. As was previously mentioned, the default mixture models were largely based upon estimation schemes or unpublished models.[29, 30] The new measurements completed as part of this project were combined with modern computational tools to improve existing models and develop new models where needed. A detailed treatment of the modeling efforts has been published separately.[27, 28] Therefore, in this work we have focused on comparisons with the default mixture models included in REFPROP (Version 10.0)[30] in an effort to provide additional context for the modeling results. Relative deviations were calculated according to eq 3. The results have been tabulated in Tables 3–10 and are also shown in Figures 4–7 plotted as percent deviation vs temperature (a), pressure (b), and density (c). Results for R-32 + R-1234yf are shown in Figure 4, R-32 + R-1234ze(E) are shown in Figure 5, R-1234yf + R-152a are shown in Figure 6, and R-1234ze(E) + R-227ea are shown in Figure 7. In each graph,

the two compositions are distinguished by separate markers, with the $x_1 \approx 0.3$ molar blend represented by circles and the $x_1 \approx 0.7$ molar blend represented by squares. Additionally, different physical states are distinguished by separate colors, with vapor-phase data shown in black, liquid-phase data shown in red, and data above the corresponding critical temperature shown in blue. For reference, smoothed curves representing the estimated combined, expanded uncertainty for each binary mixture are also shown (dashed lines). Where necessary, graph insets show vapor-phase data in greater detail.

The mixture model included in REFPROP (Version 10.0)[30] for R-32 + R-1234yf utilizes the EoS published by Tillner-Roth and Yokozeki[44] for R-32, the EoS published by Richter et al.[41] for R-1234yf, and the binary interaction parameters published by Akasaka.[45] For R-32 + R-1234ze(E), REFPROP[30] utilizes the Tillner-Roth and Yokozeki[44] EoS for R-32, the Thol and Lemmon[46] EOS for R-1234ze(E), and binary interaction parameters published by Akasaka.[45] For R-1234yf + R-152a, REFPROP[30] utilizes the Richter et al. EoS for R-1234yf,[41] the Outcalt and McLinden[47] EoS for R-152a, and the binary interaction parameters published by Bell and Lemmon.[48] Finally, for R-1234ze(E) + R-227ea, REFPROP[30] utilizes the Thol and Lemmon[46] EoS for R-1234ze(E) and the Lemmon and Span[49] EoS for R-227ea. Previously, there were no binary interaction parameters published in the literature for R-1234ze(E) + R-227ea. Instead, REFPROP[30] utilizes the binary interaction parameters for R-1234yf + R-227ea published by Bell and Lemmon.[48] However, as a result of the work done in this project, binary interaction parameters for R-1234ze(E) + R-227ea have now been reported.[27, 28]

The average absolute deviation (AAD) and the maximum absolute deviation (MAD) have been calculated to aid in the comparisons our experimental data with default mixture models. Specifically, AAD was calculated as

$$\text{AAD} = 100 \cdot \left\{ \frac{1}{N} \sum_{i=0}^{N} \left| \frac{\rho_{\text{exp},i} - \rho_{\text{REF},i}}{\rho_{\text{REF},i}} \right| \right\}, \quad (6)$$

and MAD as

$$\text{MAD} = \max \left\{ 100 \cdot \left| \frac{\rho_{\text{exp},i} - \rho_{\text{REF},i}}{\rho_{\text{REF},i}} \right| \right\} \quad (7)$$

where $\rho_{\text{exp},i}$ is the i^{th} experimental density value, $\rho_{\text{REF},i}$ is the i^{th} density value calculated using REFPROP,[30] and N is the total number of data points. The overall AAD and MAD for each of the four binary mixtures are listed in Table 11. It is clear from the data in Table 11 that the R-32 + R-1234yf mixture shows the best agreement with current mixture models with an AAD of 0.368%. The R-32 + R-1234ze(E) mixture shows the worst agreement with an AAD of 0.445%

Additionally, there are three key observations to be made from the data presented in Figures 4–7. First, in general, the measured densities in both the vapor and supercritical states are lower than the densities calculated with REFPROP,[30] while measured liquid densities are more mixed. One notable exception is the R-32 + R-1234yf mixture where a significant fraction of both liquid and supercritical data points exhibit densities higher than calculated values. Second, unsurprisingly, the worst deviations are observed for near-supercritical and supercritical state points. Whereas, overall, the AADs for the vapor-phase measurements range from 0.020% to 0.343%, the liquid-phase AADs range from 0.255% to 0.886%, while the supercritical AADs range from 0.331% to 1.034%. Finally, the observed deviations exceed estimated experimental uncertainties for all but some vapor-phase measurements. Specifically, the x_1 = 0.33512 molar composition of the R-32 + R-1234ze(E) mixture, both compositions of the R-1234yf + R-152a mixture, and both compositions of the R-1234ze(E) + R-227ea mixture exhibit deviations that are within average experimental uncertainties.

Comparisons have also been made to available literature data for the R-32 + R-1234yf, the R-32 + R-1234ze(E), and the R-1234yf + R-152a mixtures; no data were available in the literature

for the R-1234ze(E) + R-227ea mixture. Deviations relative to the corresponding default REFPROP[30] models were calculated according to eq 3 for all available literature data; the results are shown in Figures 8 and 9, plotted as a function of temperature (Figure 8) and of composition (Figure 9). For the experimental results from this work, the two compositions for each blend are still distinguished by separate markers, but no distinction is made between the different physical states. For the literature data, no symbol or color distinction is made for differences in composition; instead Figure 9 demonstrates the range of compositions for which data is available. Additionally, in Figure 8, the shaded yellow region shown in each graph designates the range of corresponding critical temperatures for each reported mixture. Where needed for clarity, particular regions have been enlarged and shown in graph insets. The overall AAD and MAD have been determined for each data set and the results are listed in Table 11.

There are several observations to be made from the data shown in Figures 8 and 9 and Table 11. First and foremost, results from this work are generally in agreement with existing literature data, and even show somewhat better agreement with default mixing models than almost half of the available data sets. The two most conspicuous outliers are the data of Kobayashi et al.[50] for R-32 + R-1234yf and Kobayashi et al.[51] for R-32 + R-1234ze(E). However, since it is clear from both Figure 8a and Figure 8b that the measurements in question were primarily made near the critical point, the large observed deviations are not unexpected. Additionally, as was observed with the data reported in this work, the literature values are generally lower than densities calculated with REFPROP,[30] except when near the critical point; the gas-phase measurements of Tomassetti[52] for R-1234yf + R-152a are the one clear exception. Finally, while the measurement results from this work nicely complement existing data sets for both R-32 + R-1234yf and R-32 + R-1234ze(E) in terms of temperature, pressure, density, and composition, they represent a significant expansion

of the available literature data for both R-1234yf + R-152a and R-1234ze(E) + R-227ea. For the former, only a single data set covering a limited range in both pressure and density was previously available, while no data was available for the latter.

Although we have focused on comparisons with the default mixture models included in REFPROP (Version 10.0),[30] it is worth noting that we have also compared the experimental data reported here with updated mixture models developed as part of this project. The updated mixture models incorporated new binary interaction parameters[27, 28] developed with the aid of the density data presented here, as well as previously-mentioned VLE and speed of sound data.[23-26] They also incorporated a new R-1234yf EoS published by Lemmon and Akasaka.[53] The resulting AADs and MADs are tabulated in Table 12 for reference; results of comparisons with available literature data are discussed by Bell.[28] In all cases, the new mixture models show a significant improvement over the default models in terms of AADs; an improvement in terms of MAD is also observed for all but the R-32 + R-1234yf blend. In particular, the observed improvement for the R-1234ze(E) + R-227ea blend is not surprising given the earlier discussion regarding the lack of binary interaction parameters and general dearth of available experimental data for this mixture.

4. Conclusions

The (p-ρ-T-x) measurement results for the four refrigerant blends R-32 + R-1234yf, R-32 + R-1234ze(E), R-1234yf + R-152a, and R-1234ze(E) + R-227ea have been reported in this work. The measurements covered temperatures from (230 to 400) K and pressures up to 22 MPa and were conducted using a two-sinker densimeter with a magnetic suspension coupling. These temperatures and pressures covered densities from approximately (2 to 1556) kg·m^{-3} and included vapor, liquid, and supercritical state points. Data comparisons show generally good agreement

with available literature data for the R-32 + R-1234yf,[50, 54-58] R-32 + R-1234ze(E),[51, 59-62] and R-1234yf + R-152a[52] blends; no data could be found for the R-1234ze(E) + R-227ea blend. Comparisons with default mixture models included in REFPROP (Version 10.0)[30] showed AADs ranging from 0.368% to 0.445% for the data presented here; in comparison, AADs for available literature data ranged from 0.166% to 3.750%. In all but one instance, the largest observed deviations were for supercritical state points. The accurate density data presented here complement existing data sets for both R-32 + R-1234yf and R-32 + R-1234ze(E), and significantly expand the available literature data for both R-1234yf + R-152a and R-1234ze(E) + R-227ea. As such, these data are invaluable to ongoing modeling efforts aimed at improving refrigerant mixture models to be made available with future versions of REFPROP.[27, 28, 30]

Acknowledgments

The authors thank our NIST colleagues Dr. Megan Harries and Dr. Jason Widegren for providing compositional analysis of the pure fluids utilized in the preparation of the measured mixtures, Dr. Aaron Rowane for assistance in mixture preparation, and Dr. Ian Bell for providing relevant available literature data. This work was supported by the U.S. Department of Energy, Building Technologies Office under Agreement 892434-19-S-EE000031.

Associated Content

Replicate density determinations at each of the (T, p) state points measured in this study are included in Tables S1–S8 of the Supporting Information file, which is available free of charge at https://pubs.acs.org/doi/101021/acs.jced.xxx. The replicate data presented in Tables S1–S8, as

well as the averaged data presented in Tables 3–10, are available for download as tab-delimited text files at https://doi.org/10.18434/mds2-2779.

References

(1) *Montreal Protocol on Substances that Deplete the Ozone Layer*; United Nations: New York, NY, USA, 1987.

(2) *Handbook for the Montreal Protocol on Substances that Deplete the Ozone Layer*; United Nations Environment Programme (UNEP) Ozone Secretariat: Nairobi, Kenya, 2020.

(3) Calm, J. M. The Next Generation of Refrigerants - Historical Review, Considerations, and Outlook. *Int. J. Refrig.* **2008**, *31*, 1123-1133.

(4) Forster, P.; Ramaswamy, V.; Artaxo, P.; Berntsen, T.; Betts, R.; Fahey, D. W.; Haywood, J.; Lean, J.; Lowe, D. C.; Myhre, G.; Nganga, J.; Prinn, R.; Raga, G.; Schulz, M.; Van Dorland, R. Changes in Atmospheric Constituents and in Radiative Forcing. In *Climate Change 2007: The Physical Science Basis. Contribution of Working Group I to the Fourth Assessment Report of the Intergovernmental Panel on Climate Change*; Solomon, S., Qin, D., Manning, M., Chen, Z., Marquis, M., Averyt, K. B., Tignor, M., Miller, H. L., Eds.; Cambridge University Press: New York, NY, USA, 2007.

(5) *Inventory of U.S. Greenhouse Gas Emissions and Sinks: 1990-2020*; EPA 430-R-22-003; U.S. Environmental Protection Agency: Washington, DC, USA, 2022.

(6) *Climate Change 2021: The Physical Science Basis. Contribution of Working Group I to the Sixth Assessment Report of the Intergovernmental Panel on Climate Change*; Masson-Delmotte, V., Zhai, P., Pirani, A., Connors, S. L., Péan, C., Berger, S., Caud, N., Chen, Y., Goldfarb, L., Gomis, M. I., Huang, M., Leitzell, K., Lonnoy, E., Matthews, J. B. R., Maycock, T. K., Waterfield, T., Yelekçi, O., Yu, R., Zhou, B., Eds.; Cambridge University Press: New York, NY, USA, 2021.

(7) *Kyoto Protocol to the United Nations Framework Convention on Climate Change*; United Nations: New York, NY, USA, 1997.

(8) Directive 2006/40/EC of the European Parliament and of the Council of 17 May 2006 Relating to Emissions from Air-Conditioning Systems in Motor Vehicles and Amending Council Directive 70/156/EEC. *Official J. Eur. Union* **2006**, L 161, 14.6.2006, 12.

(9) Regulation (EC) No 842/2006 of the European Parliament and of the Council of 17 May 2006 on Certain Fluorinated Greenhouse Gases. *Official J. Eur. Union* **2006**, L161, 14.6.2006, 1.

(10) Regulation (EU) No 517/2014 of the European Parliament and of the Council of 16 April 2014 on Fluorinated Greenhouse Gases and Repealing Regulation (EC) No 842/2006. *Official J. Eur. Union* **2014**, L 150, 20.5.2014, 195.

(11) U. S. Environmental Protection Agency. Significant New Alternatives Policy (SNAP) Regulations, https://www.epa.gov/snap/snap-regulations (accessed July 8, 2022).

(12) *Kigali Amendment to the Montreal Protocol on Substances that Deplete the Ozone Layer*; United Nations: New York, NY, USA, 2016.

(13) Bell, I. H.; Domanski, P. A.; McLinden, M. O.; Linteris, G. T. The Hunt for Nonflammable Refrigerant Blends to Replace R-134a. *Int. J. Refrig.* **2019**, *104*, 484-495.

(14) Domanski, P. A.; Brignoli, R.; Brown, J. S.; Kazakov, A. F.; McLinden, M. O. Low-GWP Refrigerants for Medium and High-Pressure Applications. *Int. J. Refrig.* **2017**, *84*, 198-209.

(15) McLinden, M. O.; Brown, J. S.; Brignoli, R.; Kazakov, A. F.; Domanski, P. A. Limited Options for Low-Global-Warming-Potential Refrigerants. *Nat. Commun.* **2017**, *8*, 14476.

(16) McLinden, M. O.; Kazakov, A. F.; Brown, J. S.; Domanski, P. A. A Thermodynamic Analysis of Refrigerants: Possibilities and Tradeoffs for Low-GWP Refrigerants. *Int. J. Refrig.* **2014**, *38*, 80-92.

(17) Hodnebrog, Ø.; Aamaas, B.; Fuglestvedt, J. S.; Marston, G.; Myhre, G.; Nielsen, C. J.; Sandstad, M.; Shine, K. P.; Wallington, T. J. Updated Global Warming Potentials and Radiative Efficiencies of Halocarbons and Other Weak Atmospheric Absorbers. *Rev. Geophys.* **2020**, *58*, e2019RG000691.

(18) Lee, Y.; Jung, D. A Brief Performance Comparison of R1234yf and R134a in a Bench Tester for Automobile Applications. *Appl. Therm. Eng.* **2012**, *35*, 240-242.

(19) Navarro-Esbrí, J.; Mendoza-Miranda, J. M.; Mota-Babiloni, A.; Barragán-Cervera, A.; Belman-Flores, J. M. Experimental Analysis of R1234yf as a Drop-In Replacement for R134a in a Vapor Compression System. *Int. J. Refrig.* **2013**, *36*, 870-880.

(20) Mota-Babiloni, A.; Navarro-Esbrí, J.; Barragán, Á.; Molés, F.; Peris, B. Drop-In Energy Performance Evaluation of R1234yf and R1234ze(E) in a Vapor Compression System as R134a Replacements. *Appl. Therm. Eng.* **2014**, *71*, 259-265.

(21) Koyama, S.; Takata, N.; Fukuda, S. Drop-In Experiments on Heat Pump Cycle Using HFO-1234ze(E) and Its Mixtures with HFC-32. *13th International Refrigeration and Air Conditioning Conference*; West Lafayette, IN, USA, July 12-15, 2010.

(22) *ANSI/ASHRAE Standard 34-2019 Designation and Safety Classification of Refrigerants*; American Society of Heating, Refrigeration and Air-Conditioning Engineers: Atlanta, GA, USA, 2019.

(23) Outcalt, S. L.; Rowane, A. J. Bubble Point Measurements of Mixtures of HFO and HFC Refrigerants. *J. Chem. Eng. Data* **2021**, *66*, 4670-4683.

(24) Outcalt, S. L.; Rowane, A. J. Bubble Point Measurements of Three Binary Mixtures of Refrigerants: R-32/1234yf, R-32/1234ze(E) and R1132a/1234yf. *J. Chem. Eng. Data* **2022**, *67*, 932-940.

(25) Rowane, A. J.; Perkins, R. A. Speed of Sound Measurements of Binary Mixtures of Hydrofluorocarbons [Pentafluoroethane (R-125), 1,1-Difluoroethane (R-152a), or 1,1,1,2,3,3,3-Heptafluoropropane (R-227ea)] with Hydrofluoroolefins [2,3,3,3-Tetrafluoropropene (R-1234yf) or *trans*-1,3,3,3-Tetrafluoropropene (R-1234ze(E))]. *Int. J. Thermophys.* **2022**, *43*, 127.

(26) Rowane, A. J.; Perkins, R. A. Speed of Sound Measurements of Binary Mixtures of Difluoromethane (R-32) with 2,3,3,3-Tetrafluoropropene (R-1234yf) or *trans*-1,3,3,3-Tetrafluoropropene (R-1234ze(E)) Refrigerants. *Int. J. Thermophys.* **2022**, *43*, 46.

(27) Bell, I. H. Mixture Models for Refrigerants R-1234yf/134a, R-1234yf/1234ze(E), and R-134a/1234ze(E) and Interim Models for R-125/1234yf, R-1234ze(E)/227ea, and R-1234yf/152a. *J. Phys. Chem. Ref. Data* **2022**, *51*, 013103.

(28) Bell, I. H. Mixture Model for Refrigerant Pairs R-32/1234yf, R-32/1234ze(E), R-1234ze(E)/227ea, R-1234yf/152a, and R-125/1234yf. *J. Phys. Chem. Ref. Data* **2023**, *52*, 013101.

(29) Bell, I. H.; Riccardi, D.; Bazyleva, A.; McLinden, M. O. Survey of Data and Models for Refrigerant Mixtures Containing Halogenated Olefins. *J. Chem. Eng. Data* **2021**, *66*, 2335-2354.

(30) Lemmon, E. W.; Bell, I. H.; Huber, M. L.; McLinden, M. O. *NIST Standard Reference Database 23: Reference Fluid Thermodynamic and Transport Properties (REFPROP)*, 10.0; National Institute of Standards and Technology: Gaithersburg, MD, USA, 2018.

(31) Piao, C.-C.; Taira, S.; Moriwaki, M.; Tanimoto, K.; Mochizuki, K.; Nakai, A. Alternatives to High GWP HFC Refrigerants: Residential and Small Commercial Unitary Equipment. *ASHRAE/NIST Refrigerants Conference*; Gaithersburg, MD, USA, Oct. 29-30, 2012.

(32) Wan, T.; Dou, Y.; Wang, L.; Yang, L.; Zhou, X.; Wan, D.; Hu, J. Environmental Benefits for Phase-Out HCFC-22 in the Residential Air-Conditioner Sector in China. *Adv. Clim. Chang. Res.* **2011**, *2*, 86-92.

(33) Maiorino, A.; Aprea, C.; Gesú Del Duca, M.; Llopis, R.; Sánchez, D.; Cabello, R. R-152a as an Alternative Refrigerant to R-134a in Domestic Refrigerators: An Experimental Analysis. *Int. J. Refrig.* **2018**, *96*, 106-116.

(34) Harris, G. L.; Torres, J. A. *Selected Laboratory and Measurement Practices and Procedures to Support Basic Mass Calibrations*; NISTIR 6969; National Institute of Standards and Technology: Gaithersburg, MD, USA, 2003.

(35) Richter, M.; McLinden, M. O. Vapor-Phase (p, ρ, T, x) Behavior and Virial Coefficients for the (Methane + Propane) System. *J. Chem. Eng. Data* **2014**, *59*, 4151-4164.

(36) Kleinrahm, R.; Wagner, W. Measurement and Correlation of the Equilibrium Liquid and Vapour Densities and the Vapour Pressure Along the Coexistence Curve of Methane. *J. Chem. Thermodyn.* **1986**, *18*, 739-760.

(37) Wagner, W.; Kleinrahm, R. Densimeters for Very Accurate Density Measurements of Fluids Over Large Ranges of Temperature, Pressure, and Density. *Metrologia* **2004**, *41*, S24-S39.

(38) McLinden, M. O.; Lösch-Will, C. Apparatus for Wide-Ranging, High-Accuracy Fluid (p-ρ-T) Measurements Based on a Compact Two-Sinker Densimeter. *J. Chem. Thermodyn.* **2007**, *39*, 507-530.

(39) McLinden, M. O.; Kleinrahm, R.; Wagner, W. Force Transmission Errors in Magnetic Suspension Densimeters. *Int. J. Thermophys.* **2007**, *28*, 429-448.

(40) Kleinrahm, R.; Yang, X.; McLinden, M. O.; Richter, M. Analysis of the Systemic Force-Transmission Error of the Magnetic-Suspension Coupling in Single-Sinker Densimeters and Commercial Gravimetric Sorption Analyzers. *Adsorption* **2019**, *25*, 717-735.

(41) Richter, M.; McLinden, M. O.; Lemmon, E. W. Thermodynamic Properties of 2,3,3,3-Tetrafluoroprop-1-ene (R1234yf): Vapor Pressure and p-ρ-T Measurements and an Equation of State. *J. Chem. Eng. Data* **2011**, *56*, 3254-3264.

(42) McLinden, M. O.; Splett, J. D. A Liquid Density Standard Over Wide Ranges of Temperature and Pressure Based on Toluene. *J. Res. Natl. Inst. Stand. Technol.* **2008**, *113*, 29-67.

(43) McLinden, M. O. Thermodynamic Properties of Propane. I. p-ρ-T Behavior from (265 to 500) K with Pressures to 36 MPa. *J. Chem. Eng. Data* **2009**, *54*, 3181-3191.

(44) Tillner-Roth, R.; Yokozeki, A. An International Standard Equation of State for Difluoromethane (R-32) for Temperatures from the Triple Point at 136.34 K to 435 K and Pressures up to 70 MPa. *J. Phys. Chem. Ref. Data* **1997**, *26*, 1273-1328.

(45) Akasaka, R. Thermodynamic Property Models for the Difluoromethane (R-32) + *trans*-1,3,3,3-Tetrafluoropropene (R-1234ze(E)) and Difluoromethane + 2,3,3,3-Tetrafluoropropene (R-1234yf) Mixtures. *Fluid Phase Equilib.* **2013**, *358*, 98-104.

(46) Thol, M.; Lemmon, E. W. Equation of State for the Thermodynamic Properties of *trans*-1,3,3,3-Tetrafluoropropene [R-1234ze(E)]. *Int. J. Thermophys.* **2016**, *37*, 28.

(47) Outcalt, S. L.; McLinden, M. O. A Modified Benedict-Webb-Rubin Equation of State for the Thermodynamic Properties of R152a (1,1-Difluoroethane). *J. Phys. Chem. Ref. Data* **1996**, *25*, 605-636.

(48) Bell, I. H.; Lemmon, E. W. Automatic Fitting of Binary Interaction Parameters for Multi-Fluid Helmholtz-Energy-Explicit Mixture Models. *J. Chem. Eng. Data* **2016**, *61*, 3752-3760.

(49) Lemmon, E. W.; Span, R. Thermodynamic Properties of R-227ea, R-365mfc, R-115, and R-1311. *J. Chem. Eng. Data* **2015**, *60*, 3745-3758.

(50) Kobayashi, K.; Tanaka, K.; Higashi, Y. Measurements of *PρTx* Properties for the Binary HFO-1234yf + HFC-32 Mixtures. *23rd IIR International Congress of Refrigeration*; Prague, Czech Republic, August 21–26, 2011.

(51) Kobayashi, K.; Tanaka, K.; Higashi, Y. *PρTx* Property Measurements of Binary HFO-1234ze(E) + HFC-32 Refrigerant Mixtures. *Trans. JSRAE* **2011**, *28*, 415-426.

(52) Tomassetti, S. *pvTz* Properties of 2,3,3,3-Tetrafluoroprop-1-ene + 1,1-Difluoroethane Binary System Measured in the Two-Phase and Superheated Vapor Regions. *Fluid Phase Equilib.* **2021**, *546*, 113173.

(53) Lemmon, E. W.; Akasaka, R. An International Standard Formulation for 2,3,3,3-Tetrafluoroprop-1-ene (R1234yf) Covering Temperatures from the Triple Point Temperature to 410 K and Pressures up to 100 MPa. *Int. J. Thermophys.* **2022**, *43*, 119.

(54) Cai, X.-D.; Zhang, N.; Chen, L.-X.; Hu, P.; Zhao, G.; Liu, M.-H. Gaseous *PvTx* Measurements of HFO-1234yf + HFC-32 Binary Mixture by Single-Sinker Magnetic Suspension Densimeter. *Fluid Phase Equilib.* **2018**, *460*, 119-125.

(55) Dang, Y.; Kamiaka, T.; Dang, C.; Hihara, E. Liquid Viscosity of Low-GWP Refrigerant Mixtures (R32 + R1234yf) and (R125 + R1234yf). *J. Chem. Thermodyn.* **2015**, *89*, 183-188.

(56) Jia, X.; Yang, J.; Wu, J. Compressed Liquid Densities of Binary Mixtures of Difluoromethane (R32) and 2,3,3,3-Tetrafluoroprop-1-ene (R1234yf) at Temperatures from (283 to 363) K and Pressures up to 100 MPa. *J. Chem. Thermodyn.* **2020**, *141*, 105935.

(57) Tomassetti, S.; Coccia, G.; Pierantozzi, M.; Di Nicola, G.; Brown, J. S. Vapor Phase and Two-Phase *PvTz* Measurements of Difluoromethane + 2,3,3,3-Tetrafluoroprop-1-ene. *J. Chem. Thermodyn.* **2020**, *141*, 105966.

(58) Yang, J.; Jia, X.; Wu, J. Vapor Phase *pvTx* Measurements of Binary Mixtures of Difluoromethane (R32) and 2,3,3,3-Tetrafluoroprop-1-ene (R1234yf). *J. Chem. Thermodyn.* **2019**, *134*, 41-51.

(59) Jia, T.; Bi, S.; Hu, X.; Meng, X.; Wu, J. Volumetric Properties of Binary Mixtures of {Difluoromethane (R32) + *trans*-1,3,3,3-Tetrafluoropropene (R1234ze(E))} at Temperatures from 283.15 K to 363.15 K and Pressures up to 100 MPa. *J. Chem. Thermodyn.* **2016**, *101*, 54-63.

(60) Tanaka, K.; Akasaka, R.; Higashi, Y. Measurements of Density and Isobaric Specific Heat Capacity for HFO-1234ze(E)+HFC-32 Mixtures. *Trans. JSRAE* **2011**, *28*, 427-434.

(61) Tomassetti, S.; Perera, U. A.; Di Nicola, G.; Pierantozzi, M.; Higashi, Y.; Thu, K. Two-Phase and Vapor-Phase Thermophysical Property (*pvTz*) Measurements of the Difluoromethane + *trans*-1,3,3,3-Tetrafluoroprop-1-ene Binary System. *J. Chem. Eng. Data* **2020**, *65*, 1554-1564.

(62) Yamaya, K.; Matsuguchi, A.; Kagawa, N. Study on the Isochoric Specific Heat Capacity of a R32+R1234ze(E) Mixture in the Liquid Phase. *23rd IIR International Congress of Refrigeration*; Prague, Czech Republic, August 21–26, 2011.

(63) Hanwell, M. D.; Curtis, D. E.; Lonie, D. C.; Vandermeersch, T.; Zurek, E.; Hutchison, G. R. Avogadro: An Advanced Semantic Chemical Editor, Visualization, and Analysis Platform. *J. Cheminform.* **2012**, *4*, 17.

Table 1. Chemical Information

Refrigerant	Chemical Name	Chemical Formula	CAS	Supplier[a]	Purity[b]
R-32	difluoromethane	CH_2F_2	75-10-5	Advanced Specialty Gas	0.999
R-152a	1,1-difluoroethane	$C_2H_4F_2$	75-37-6	Chemours	0.9994
R-227ea	1,1,1,2,3,3,3-heptafluoropropane	C_3HF_7	431-89-0	Honeywell	0.9997
R-1234yf	2,3,3,3-tetrafluoropropene	$C_3H_2F_4$	754-12-1	Chemours	0.999
R-1234ze(E)	*trans*-1,3,3,3-tetrafluoropropene	$C_3H_2F_4$	29118-24-9	Honeywell	0.9997

[a]In order to describe materials and experimental procedures adequately, it is occasionally necessary to identify commercial products by manufacturers' names or labels. In no instance does such identification imply endorsement by the National Institute of Standards and Technology, nor does it imply that the particular product or equipment is necessarily the best available for the purpose. [b]Supplier's stated purity in mole fraction.

Table 2. Measured Refrigerant Blends

Blend	x_1[a]	x_2[a]	Sample Volume
R-32 + R-1234yf	0.33681	0.66319	6 L
	0.67205	0.32795	6 L
R-32 + R-1234ze(E)	0.33512	0.66488	10 L
	0.66665	0.33335	10 L
R-1234yf + R-152a	0.33342	0.66658	13.4 L
	0.66526	0.33474	13.4 L
R-1234ze(E) + R-227ea	0.33265	0.66735	13.4 L
	0.66803	0.33197	13.4 L

[a]Molar composition of first (1) and second (2) component. Standard uncertainty in molar composition from gravimetric preparation estimated at 0.00005.

Table 3. Measured Temperature (T), Pressure (p), and Density (ρ) Data for the 0.33681/0.66319 Molar R-32 + R-1234yf Blend[a]

T[b] /K	p /MPa	ρ /kg·m^{-3}	$u(p)$[c] /kPa	$100\cdot(U(\rho)/\rho)$[d]	$\Delta\rho$[e]
		Vapor-phase			
293.153	0.0902	3.505	0.030	0.121	-0.041
293.150	0.1834	7.254	0.030	0.065	-0.093
293.153	0.2631	10.574	0.030	0.057	-0.132
293.153	0.3321	13.543	0.030	0.051	-0.166
293.153	0.4127	17.131	0.030	0.048	-0.206
293.153	0.4956	20.969	0.030	0.047	-0.245
293.155	0.5737	24.739	0.030	0.046	-0.281
293.151	0.6536	28.770	0.030	0.045	-0.318
293.154	0.7295	32.790	0.030	0.045	-0.350
283.163	0.0830	3.342	0.030	0.137	-0.049
283.162	0.1204	4.886	0.030	0.086	-0.073
283.162	0.1885	7.765	0.030	0.063	-0.117
283.161	0.2485	10.378	0.030	0.056	-0.156
283.163	0.3017	12.765	0.030	0.053	-0.188
283.160	0.3605	15.476	0.030	0.050	-0.224
283.162	0.4207	18.345	0.030	0.048	-0.261
283.161	0.4870	21.624	0.030	0.047	-0.300
283.162	0.5414	24.420	0.030	0.046	-0.331
283.160	0.5700	25.930	0.030	0.045	-0.348
283.161	0.5753	26.214	0.030	0.046	-0.351
283.162	0.5806	26.494	0.030	0.046	-0.354
273.152	0.0549	2.281	0.030	0.174	-0.060
273.148	0.1096	4.615	0.030	0.090	-0.097
273.148	0.1592	6.787	0.030	0.083	-0.134
273.152	0.2048	8.834	0.030	0.064	-0.166
273.150	0.2596	11.364	0.030	0.054	-0.208
273.147	0.3080	13.671	0.030	0.051	-0.246
273.147	0.3513	15.792	0.030	0.052	-0.280
273.150	0.3808	17.274	0.030	0.048	-0.301
273.149	0.3901	17.746	0.030	0.048	-0.308
273.148	0.3991	18.206	0.030	0.048	-0.315
273.148	0.4078	18.657	0.030	0.049	-0.323
273.149	0.4164	19.101	0.030	0.048	-0.329
263.148	0.0653	2.827	0.030	0.136	-0.089
263.149	0.0997	4.359	0.030	0.107	-0.116
263.152	0.1321	5.831	0.030	0.076	-0.143
263.152	0.1626	7.245	0.030	0.068	-0.172
263.151	0.1914	8.600	0.030	0.061	-0.200
263.149	0.2184	9.897	0.030	0.058	-0.227
263.149	0.2438	11.140	0.030	0.058	-0.253
263.148	0.2560	11.745	0.030	0.054	-0.265
263.147	0.2794	12.918	0.030	0.053	-0.290
263.148	0.2906	13.484	0.030	0.051	-0.303
253.144	0.0604	2.723	0.030	0.142	-0.107

253.144	0.0935	4.260	0.030	0.098	-0.144
253.142	0.1093	5.005	0.030	0.087	-0.163
253.143	0.1246	5.735	0.030	0.084	-0.181
253.146	0.1538	7.154	0.030	0.069	-0.218
253.146	0.1678	7.842	0.030	0.065	-0.235
253.144	0.1813	8.516	0.030	0.062	-0.254
253.142	0.1944	9.174	0.030	0.060	-0.274
Liquid-phase and supercritical states					
230.122	1.2288	1273.424	1.560	0.044	-0.212
240.122	1.5447	1246.320	1.660	0.045	-0.188
240.120	1.5402	1246.312	1.640	0.044	-0.188
240.119	1.5599	1246.370	1.750	0.045	-0.188
240.121	1.5578	1246.357	1.310	0.044	-0.188
240.122	1.5543	1246.344	1.780	0.045	-0.188
240.120	1.5707	1246.396	3.710	0.054	-0.188
255.119	7.7218	1222.360	5.220	0.064	-0.195
255.124	6.3685	1218.251	2.040	0.045	-0.180
255.123	5.0487	1214.132	1.670	0.044	-0.166
255.121	2.6758	1206.373	1.310	0.044	-0.136
255.121	1.7880	1203.338	1.100	0.043	-0.124
265.122	9.1513	1199.163	1.670	0.044	-0.162
265.123	6.6488	1190.740	1.670	0.044	-0.132
265.126	4.4089	1182.690	1.490	0.044	-0.102
265.125	3.3592	1178.735	1.410	0.044	-0.087
265.125	2.3644	1174.863	1.290	0.044	-0.071
275.124	9.1824	1171.001	1.520	0.044	-0.105
275.124	6.9937	1162.634	1.540	0.044	-0.074
275.126	4.9939	1154.460	1.340	0.044	-0.043
275.123	3.1698	1146.500	1.320	0.044	-0.011
275.124	2.3190	1142.588	1.160	0.043	0.006
285.126	8.5403	1138.943	1.110	0.043	-0.026
285.127	5.8025	1126.475	1.280	0.043	0.023
285.126	4.1508	1118.274	1.380	0.044	0.058
285.126	1.9603	1106.397	1.320	0.044	0.111
295.130	7.5712	1103.003	1.190	0.043	0.076
295.129	6.0111	1094.545	1.240	0.043	0.113
295.129	3.9279	1082.183	1.190	0.043	0.169
295.129	2.1107	1070.146	1.140	0.043	0.229
310.135	9.7012	1065.691	1.160	0.043	0.167
310.136	7.6692	1052.727	1.240	0.043	0.226
310.137	5.8778	1039.957	1.200	0.043	0.289
310.136	3.8255	1023.237	1.130	0.043	0.379
310.136	2.1087	1006.818	1.130	0.043	0.476
325.145	8.4069	1003.007	1.090	0.043	0.375
325.145	6.5362	985.663	1.140	0.043	0.471
325.145	4.6164	964.343	1.090	0.043	0.606
325.146	2.5718	934.966	1.210	0.043	0.835
340.156	7.6164	931.645	1.070	0.043	0.646
340.157	6.1183	909.852	1.110	0.043	0.808

340.162	5.1368	892.455	1.260	0.044	0.962
340.158	3.5297	853.891	1.060	0.043	1.423
355.155	7.4395	851.089	1.080	0.044	0.998
355.155	7.0411	842.151	1.090	0.044	1.080
355.155	6.0576	815.832	1.100	0.044	1.360
355.155	5.0297	776.630	1.060	0.044	1.917
355.155	4.5720	750.534	1.050	0.044	2.440
370.152	7.3795	747.207	1.040	0.044	1.546
370.155	6.5185	703.630	1.070	0.044	2.079
370.155	6.0485	668.321	1.050	0.044	2.606
370.155	5.5439	607.038	1.040	0.044	-2.355
370.156	5.0349	467.734	1.060	0.044	-1.317
400.151	7.5365	465.945	1.060	0.044	-0.999
400.156	6.5076	355.749	1.070	0.044	-0.531
400.154	5.9962	303.585	1.200	0.044	-0.395
400.155	5.4705	256.024	1.080	0.044	-0.287
400.154	4.9784	217.476	1.090	0.052	0.338
400.154	3.9753	153.595	1.090	0.060	0.015
400.155	2.8634	98.929	1.100	0.077	-0.163
400.155	1.8674	59.339	1.190	0.131	-0.256

[a]Reported values are averages of replicate measurements at each (T, p) state point. [b]Standard uncertainty in temperature is 3 mK. [c]Standard uncertainty in pressure. [d]Relative combined, expanded (k = 2) state-point uncertainty in density. [e]Relative deviation from default mixing model calculated according to eq 3.

Table 4. Measured Temperature (T), Pressure (p), and Density (ρ) Data for the 0.67205/0.32795 Molar R-32 + R-1234yf Blend[a]

T[b] /K	p /MPa	ρ /kg·m^{-3}	$u(p)$[c] /kPa	100·($U(\rho)/\rho$)[d]	$\Delta\rho$ [e]
Vapor-phase					
293.155	0.1175	3.550	0.030	0.102	-0.078
293.155	0.2170	6.659	0.030	0.065	-0.145
293.155	0.3043	9.474	0.030	0.060	-0.205
293.157	0.4170	13.235	0.030	0.051	-0.285
293.154	0.5114	16.506	0.030	0.049	-0.355
293.152	0.6024	19.776	0.030	0.047	-0.425
293.155	0.7050	23.617	0.030	0.047	-0.508
293.155	0.8037	27.479	0.030	0.046	-0.591
293.152	0.9010	31.476	0.040	0.046	-0.681
293.155	0.9779	34.779	0.040	0.046	-0.754
283.152	0.0818	2.551	0.030	0.144	-0.052
283.153	0.1801	5.712	0.030	0.073	-0.132
283.151	0.2666	8.590	0.030	0.058	-0.204
283.150	0.3607	11.836	0.030	0.054	-0.285
283.152	0.4715	15.828	0.030	0.050	-0.385
283.150	0.5621	19.243	0.030	0.048	-0.471
283.150	0.6620	23.186	0.030	0.047	-0.574
283.153	0.7647	27.469	0.030	0.046	-0.688
273.169	0.0703	2.270	0.030	0.174	-0.093
273.170	0.1394	4.565	0.030	0.084	-0.144
273.169	0.2222	7.401	0.030	0.063	-0.221
273.170	0.3286	11.208	0.030	0.053	-0.328
273.170	0.4312	15.067	0.030	0.051	-0.442
273.169	0.5266	18.852	0.030	0.048	-0.559
273.168	0.5575	20.122	0.030	0.048	-0.600
263.180	0.0625	2.095	0.030	0.164	-0.114
263.181	0.1072	3.631	0.030	0.103	-0.149
263.179	0.1700	5.843	0.030	0.073	-0.212
263.179	0.2089	7.249	0.030	0.067	-0.257
263.181	0.2628	9.248	0.030	0.058	-0.325
263.180	0.3121	11.126	0.030	0.054	-0.392
263.178	0.3572	12.892	0.030	0.054	-0.459
263.177	0.3852	14.012	0.030	0.051	-0.502
253.159	0.0561	1.954	0.030	0.175	-0.163
253.161	0.0991	3.493	0.030	0.103	-0.189
253.160	0.1394	4.970	0.030	0.086	-0.236
253.159	0.1587	5.688	0.030	0.074	-0.261
253.158	0.1955	7.082	0.030	0.065	-0.316
253.157	0.2130	7.759	0.030	0.063	-0.345
253.155	0.2300	8.420	0.030	0.059	-0.373
253.155	0.2624	9.704	0.030	0.057	-0.434
253.157	0.2779	10.326	0.030	0.057	-0.463
Liquid-phase and supercritical states					
230.149	1.7740	1238.825	1.300	0.045	-0.278

240.157	2.2303	1211.376	6.590	0.061	-0.255
240.157	2.2452	1211.420	4.560	0.052	-0.255
240.157	2.2444	1211.412	4.180	0.051	-0.256
240.157	2.2459	1211.428	5.250	0.054	-0.255
255.152	14.0530	1199.842	2.920	0.047	-0.293
255.150	12.3923	1195.644	2.420	0.046	-0.282
255.150	9.4124	1187.759	2.090	0.046	-0.260
255.151	7.9837	1183.805	1.890	0.045	-0.248
255.151	5.4161	1176.384	1.910	0.045	-0.225
255.151	4.2004	1172.715	1.330	0.045	-0.213
255.150	2.6375	1167.836	1.350	0.045	-0.197
265.159	10.4614	1162.441	1.920	0.045	-0.224
265.161	9.1277	1158.340	1.720	0.045	-0.212
265.157	7.8767	1154.385	1.170	0.044	-0.200
265.161	5.5992	1146.823	1.300	0.044	-0.176
265.161	3.5297	1139.538	1.260	0.044	-0.152
265.160	2.6620	1136.347	1.350	0.045	-0.141
275.149	10.0073	1131.754	2.000	0.045	-0.168
275.149	8.8495	1127.645	1.920	0.045	-0.155
275.149	6.7591	1119.856	1.340	0.044	-0.130
275.150	4.8409	1112.249	1.420	0.045	-0.105
275.150	2.5271	1102.367	6.030	0.057	-0.071
284.998	8.9633	1097.376	1.580	0.045	-0.095
284.999	8.0103	1093.336	1.500	0.045	-0.081
285.000	6.2547	1085.525	1.340	0.044	-0.055
285.002	3.8994	1074.154	1.310	0.044	-0.015
284.999	2.6492	1067.629	1.210	0.044	0.009
295.002	8.6533	1063.076	1.350	0.044	-0.018
295.000	7.0921	1055.077	1.500	0.045	0.010
295.002	5.0082	1043.437	1.260	0.044	0.053
295.004	2.6999	1028.930	1.470	0.045	0.111
309.983	10.8065	1022.906	1.210	0.044	0.058
309.986	8.7979	1010.551	1.480	0.045	0.103
309.985	7.0210	998.400	1.220	0.044	0.150
309.986	4.9869	982.594	1.230	0.044	0.215
309.988	2.6209	960.484	2.690	0.047	0.316
324.994	9.3446	955.448	1.150	0.044	0.228
324.995	7.9844	943.066	1.110	0.044	0.279
324.996	6.0708	922.767	1.170	0.044	0.373
324.997	4.0130	894.916	1.110	0.044	0.524
324.995	3.1071	879.219	1.060	0.044	0.626
340.010	8.2989	873.691	1.210	0.045	0.458
340.009	8.2769	873.385	1.170	0.044	0.460
340.004	7.3347	858.837	0.630	0.044	0.545
340.004	6.0156	833.724	0.550	0.044	0.698
340.004	5.0227	808.676	0.450	0.044	0.887
340.003	4.3101	784.081	0.490	0.044	1.121
359.999	9.6134	780.172	0.360	0.044	0.629
359.999	7.8325	726.829	0.410	0.044	0.904
360.001	6.8106	674.041	0.360	0.044	1.163

360.001	6.0708	595.377	0.350	0.044	1.334
379.996	9.1139	593.289	0.340	0.044	0.681
379.998	7.9196	485.437	0.380	0.044	0.176
379.998	6.9131	352.559	0.380	0.044	0.402
379.998	5.9602	248.653	0.410	0.044	0.598
379.997	4.9076	172.685	0.440	0.046	-1.071
399.996	5.5003	172.285	0.450	0.047	-0.856
399.997	4.9429	147.461	0.460	0.047	-0.775
399.997	3.6578	98.750	0.460	0.050	-0.577
400.000	2.8244	72.042	0.480	0.056	-0.455
399.995	2.0320	49.358	0.570	0.096	-0.293
399.999	1.5668	37.020	0.270	0.074	-0.278

[a]Reported values are averages of replicate measurements at each (T, p) state point. [b]Standard uncertainty in temperature is 3 mK. [c]Standard uncertainty in pressure. [d]Relative combined, expanded (k = 2) state-point uncertainty in density. [e]Relative deviation from default mixing model calculated according to eq 3.

Table 5. Measured Temperature (T), Pressure (p), and Density (ρ) Data for the 0.33512/0.66488 Molar R-32 + R-1234ze(E) Blend[a]

T[b] /K	p /MPa	ρ /kg·m^{-3}	$u(p)$[c] /kPa	100·($U(\rho)/\rho$)[d]	$\Delta\rho$ [e]
		Vapor-phase			
293.150	0.1397	5.496	0.030	0.084	-0.052
293.150	0.2021	8.054	0.030	0.061	-0.064
293.150	0.2659	10.742	0.030	0.057	-0.070
293.151	0.3280	13.441	0.030	0.051	-0.071
293.151	0.3861	16.042	0.030	0.049	-0.067
293.151	0.4437	18.695	0.030	0.047	-0.057
293.152	0.5032	21.532	0.030	0.046	-0.039
293.153	0.5401	23.339	0.030	0.046	-0.023
293.150	0.5427	23.468	0.030	0.046	-0.022
293.148	0.5452	23.594	0.030	0.046	-0.021
293.149	0.5477	23.718	0.030	0.046	-0.020
293.151	0.5502	23.840	0.030	0.046	-0.019
293.153	0.5526	23.960	0.030	0.046	-0.017
293.150	0.5549	24.077	0.030	0.046	-0.016
293.148	0.5572	24.191	0.030	0.046	-0.016
293.150	0.5594	24.301	0.030	0.046	-0.014
293.152	0.5615	24.409	0.030	0.046	-0.013
293.151	0.5636	24.514	0.030	0.046	-0.012
293.148	0.5657	24.617	0.030	0.046	-0.011
293.148	0.5677	24.719	0.030	0.045	-0.010
293.149	0.5697	24.819	0.030	0.046	-0.009
293.153	0.5716	24.917	0.030	0.045	-0.009
293.152	0.5735	25.012	0.030	0.045	-0.007
293.148	0.5753	25.105	0.030	0.046	-0.007
283.156	0.0993	4.022	0.030	0.097	-0.056
283.153	0.1513	6.203	0.030	0.071	-0.060
283.153	0.2084	8.660	0.030	0.060	-0.065
283.152	0.2579	10.852	0.030	0.054	-0.068
283.152	0.3011	12.813	0.030	0.052	-0.067
283.152	0.3526	15.221	0.030	0.049	-0.058
283.151	0.3841	16.729	0.030	0.048	-0.052
283.151	0.4005	17.525	0.030	0.048	-0.046
283.149	0.4060	17.790	0.030	0.048	-0.045
283.147	0.4112	18.049	0.030	0.048	-0.043
283.147	0.4164	18.302	0.030	0.048	-0.042
273.147	0.0793	3.321	0.030	0.119	-0.064
273.146	0.1316	5.588	0.030	0.077	-0.066
273.146	0.1670	7.161	0.030	0.066	-0.069
273.146	0.2098	9.107	0.030	0.058	-0.072
273.145	0.2480	10.892	0.030	0.054	-0.070
273.147	0.2741	12.133	0.030	0.053	-0.067
273.149	0.2854	12.667	0.030	0.052	-0.114
273.149	0.2895	12.879	0.030	0.052	-0.050
273.149	0.2934	13.064	0.030	0.051	-0.065

273.157	0.0804	3.370	0.030	0.116	-0.066
273.155	0.1316	5.589	0.030	0.077	-0.066
273.152	0.1663	7.132	0.030	0.066	-0.068
273.151	0.2082	9.035	0.030	0.059	-0.070
273.151	0.2457	10.780	0.030	0.055	-0.068
273.153	0.2712	11.994	0.030	0.053	-0.065
273.155	0.2861	12.711	0.030	0.054	-0.063
273.152	0.2898	12.888	0.030	0.052	-0.063
263.153	0.0706	3.069	0.030	0.129	-0.094
263.154	0.1080	4.751	0.030	0.088	-0.087
263.154	0.1207	5.329	0.030	0.081	-0.084
263.152	0.1417	6.298	0.030	0.072	-0.085
263.153	0.1601	7.161	0.030	0.067	-0.084
263.157	0.1810	8.150	0.030	0.062	-0.083
263.156	0.1963	8.884	0.030	0.060	-0.083
253.149	0.0594	2.682	0.030	0.149	-0.097
253.146	0.0819	3.727	0.030	0.108	-0.096
253.145	0.1010	4.628	0.030	0.090	-0.093
253.145	0.1208	5.576	0.030	0.079	-0.092
253.145	0.1277	5.910	0.030	0.077	-0.093
Liquid-phase and supercritical states					
230.008	1.9251	1324.368	1.650	0.045	-0.915
230.008	1.9270	1324.374	1.830	0.045	-0.915
230.007	1.9269	1324.375	1.820	0.045	-0.915
230.009	1.9293	1324.373	1.730	0.045	-0.915
230.012	1.9311	1324.370	1.920	0.045	-0.915
230.013	1.7306	1323.962	1.670	0.045	-0.913
245.008	17.4796	1317.778	1.820	0.045	-0.967
245.012	15.2179	1313.399	1.320	0.044	-0.948
245.011	13.0621	1309.108	2.070	0.045	-0.929
245.011	9.0592	1300.773	1.710	0.044	-0.893
245.012	7.1832	1296.685	1.630	0.044	-0.874
245.011	3.6974	1288.759	1.910	0.045	-0.836
245.013	2.0847	1284.918	1.610	0.044	-0.818
259.992	16.5331	1279.915	1.550	0.044	-0.887
259.996	14.5978	1275.530	1.450	0.044	-0.869
259.994	10.9634	1266.926	1.650	0.044	-0.833
259.998	9.2633	1262.696	1.490	0.044	-0.814
259.995	6.0732	1254.413	1.520	0.044	-0.776
260.001	3.1697	1246.364	1.960	0.045	-0.737
259.996	1.8465	1242.542	1.610	0.044	-0.719
280.000	18.9215	1236.606	1.470	0.044	-0.822
280.000	17.2033	1232.053	1.630	0.044	-0.804
279.999	13.9895	1223.119	1.790	0.044	-0.769
279.998	11.0374	1214.355	1.730	0.044	-0.732
279.999	8.3264	1205.761	1.490	0.044	-0.694
280.000	4.6703	1193.167	1.580	0.044	-0.636
280.003	2.4905	1184.991	1.410	0.044	-0.595
280.001	1.7797	1182.207	1.450	0.044	-0.581

304.999	19.4579	1175.049	1.310	0.043	-0.726
305.000	16.7873	1165.837	1.320	0.043	-0.692
304.999	14.3197	1156.729	1.450	0.044	-0.657
304.998	10.9765	1143.287	1.440	0.044	-0.603
304.998	8.0216	1130.078	1.410	0.043	-0.546
304.999	5.4141	1117.086	1.330	0.043	-0.485
304.998	3.1260	1104.335	1.390	0.043	-0.420
305.001	1.7639	1095.968	1.180	0.043	-0.375
315.001	7.3165	1093.526	1.150	0.043	-0.463
325.006	12.8513	1091.294	1.280	0.043	-0.534
325.005	12.7616	1090.830	1.700	0.044	-0.532
339.997	21.0499	1088.113	1.460	0.044	-0.617
339.997	18.1690	1073.950	1.430	0.044	-0.570
339.996	14.8179	1055.323	1.280	0.043	-0.505
339.998	11.9576	1036.946	1.360	0.044	-0.435
339.998	8.9777	1014.269	1.200	0.043	-0.340
339.996	6.1400	987.396	1.340	0.044	-0.212
339.997	4.2945	965.235	1.100	0.043	-0.091
339.997	2.5715	938.314	1.140	0.043	0.074
349.995	5.9724	936.649	1.090	0.043	-0.108
360.000	9.4148	935.148	1.140	0.043	-0.250
369.998	12.8719	933.729	1.140	0.044	-0.358
379.997	16.3319	932.358	1.180	0.044	-0.440
384.997	18.0571	931.657	1.210	0.044	-0.473
384.998	17.5522	926.795	1.150	0.044	-0.464
384.998	14.8780	897.668	1.140	0.044	-0.412
384.998	12.1888	859.824	1.120	0.044	-0.357
384.999	9.0899	793.508	1.090	0.044	-0.349
389.997	10.2091	792.945	1.080	0.044	-0.389
394.997	11.3334	792.386	1.080	0.044	-0.422
400.002	12.4621	791.823	1.090	0.044	-0.447
400.002	10.4974	739.392	1.090	0.044	-0.541
400.002	8.9988	677.748	1.070	0.044	-0.850
400.001	7.5414	569.083	1.070	0.044	1.446
400.002	6.6623	451.472	1.070	0.044	1.065
400.003	5.8893	334.657	1.080	0.044	0.392
400.003	4.3435	183.399	1.100	0.055	0.002
400.003	3.3367	123.590	1.110	0.067	-0.132
400.004	2.1150	69.323	1.130	0.106	-0.292
400.004	1.4290	44.208	1.180	0.188	-0.393

[a]Reported values are averages of replicate measurements at each (T, p) state point. [b]Standard uncertainty in temperature is 3 mK. [c]Standard uncertainty in pressure. [d]Relative combined, expanded (k = 2) state-point uncertainty in density. [e]Relative deviation from default mixing model calculated according to eq 3.

Table 6. Measured Temperature (T), Pressure (p), and Density (ρ) Data for the 0.66665/0.33335 Molar R-32 + R-1234ze(E) Blend[a]

T[b] /K	p /MPa	ρ /kg·m^{-3}	$u(p)$[c] /kPa	$100\cdot(U(\rho)/\rho)$[d]	$\Delta\rho$ [e]
Vapor-phase					
293.156	0.1465	4.469	0.030	0.104	-0.072
293.155	0.3155	9.906	0.030	0.055	-0.115
293.157	0.4572	14.731	0.030	0.050	-0.145
293.159	0.6001	19.885	0.030	0.048	-0.163
293.159	0.7529	25.774	0.030	0.048	-0.163
293.158	0.8009	27.716	0.030	0.046	-0.159
293.158	0.8512	29.810	0.040	0.046	-0.151
293.157	0.8536	29.908	0.030	0.046	-0.150
293.156	0.8558	30.004	0.030	0.047	-0.149
293.157	0.8580	30.094	0.030	0.046	-0.149
293.158	0.8601	30.184	0.040	0.047	-0.148
293.158	0.8623	30.278	0.030	0.046	-0.147
293.159	0.8647	30.379	0.030	0.046	-0.147
293.156	0.8670	30.478	0.030	0.046	-0.148
293.155	0.8693	30.576	0.040	0.046	-0.148
293.155	0.8716	30.674	0.030	0.046	-0.147
283.155	0.0954	2.994	0.030	0.148	-0.057
283.158	0.2159	6.935	0.030	0.074	-0.095
283.157	0.3008	9.825	0.030	0.056	-0.122
283.155	0.4004	13.354	0.030	0.055	-0.148
283.157	0.5036	17.185	0.030	0.049	-0.165
283.156	0.5514	19.026	0.030	0.049	-0.171
283.157	0.6006	20.970	0.030	0.047	-0.175
283.157	0.6224	21.851	0.030	0.049	-0.175
273.154	0.0908	2.961	0.030	0.165	-0.072
273.153	0.1699	5.631	0.030	0.074	-0.097
273.155	0.2229	7.479	0.030	0.067	-0.115
273.156	0.2871	9.775	0.030	0.056	-0.138
273.156	0.3443	11.885	0.030	0.053	-0.156
273.155	0.4073	14.285	0.030	0.051	-0.175
273.154	0.4410	15.606	0.030	0.049	-0.185
263.156	0.0865	2.931	0.030	0.122	-0.088
263.154	0.1254	4.291	0.030	0.086	-0.101
263.154	0.1620	5.594	0.030	0.073	-0.115
263.155	0.2129	7.452	0.030	0.063	-0.140
263.155	0.2444	8.627	0.030	0.058	-0.154
263.156	0.2818	10.049	0.030	0.055	-0.172
253.151	0.0830	2.931	0.030	0.123	-0.109
253.149	0.1227	4.383	0.030	0.088	-0.128
253.152	0.1606	5.800	0.030	0.072	-0.151
253.153	0.2009	7.347	0.030	0.064	-0.182
Liquid-phase and supercritical states					
230.012	2.0048	1272.974	1.220	0.045	-1.295
230.012	2.0026	1272.972	1.250	0.045	-1.294

230.012	1.8669	1272.704	4.090	0.051	-1.292
245.006	11.8489	1253.410	2.560	0.046	-1.297
245.005	11.7902	1253.289	2.410	0.046	-1.296
245.006	11.7393	1253.180	2.220	0.046	-1.296
245.005	7.8812	1245.027	2.470	0.046	-1.253
245.007	6.1238	1241.136	2.190	0.046	-1.231
245.006	4.4717	1237.385	1.940	0.045	-1.210
245.009	2.1745	1231.973	13.070	0.088	-1.179
260.006	16.2626	1224.371	2.330	0.046	-1.251
260.010	14.3180	1219.917	2.800	0.047	-1.229
260.007	12.4818	1215.595	2.550	0.046	-1.207
260.008	9.1695	1207.413	2.330	0.046	-1.164
260.009	6.1750	1199.558	1.800	0.045	-1.121
260.009	3.4823	1192.063	1.970	0.045	-1.077
260.010	2.5087	1189.236	3.380	0.049	-1.060
280.002	19.9775	1181.885	3.450	0.048	-1.182
280.003	15.1240	1168.604	2.320	0.046	-1.119
280.003	12.2364	1160.041	1.990	0.045	-1.076
280.004	9.6028	1151.711	2.060	0.045	-1.031
280.009	6.0878	1139.659	2.210	0.046	-0.963
280.005	3.9972	1131.904	1.870	0.045	-0.916
280.009	2.2384	1124.935	1.500	0.045	-0.871
304.997	20.5738	1117.231	3.020	0.047	-1.058
305.000	19.2101	1112.512	2.850	0.046	-1.036
304.997	15.5843	1099.148	1.960	0.045	-0.972
304.999	13.3973	1090.354	1.930	0.045	-0.928
304.996	10.4542	1077.485	1.620	0.045	-0.860
304.996	7.0830	1060.835	1.400	0.044	-0.762
304.997	4.9079	1048.652	1.260	0.044	-0.683
304.995	2.4798	1033.230	1.800	0.045	-0.570
315.001	8.1027	1030.150	1.540	0.045	-0.696
325.003	13.6920	1027.306	1.680	0.045	-0.795
339.998	22.0555	1023.704	2.410	0.046	-0.916
340.001	20.2199	1014.338	2.620	0.046	-0.877
339.999	17.0059	996.185	1.740	0.045	-0.798
339.997	14.2465	978.239	1.440	0.045	-0.713
339.996	10.8845	952.042	1.330	0.045	-0.578
339.997	8.2525	926.243	1.210	0.044	-0.427
339.997	6.2249	900.831	1.160	0.044	-0.257
339.999	4.0846	863.264	1.100	0.044	0.046
349.996	7.4646	861.451	1.130	0.044	-0.247
360.000	10.8797	859.626	1.220	0.045	-0.444
360.000	9.0561	829.038	1.090	0.045	-0.324
359.999	8.0519	807.281	1.140	0.045	-0.247
359.999	7.1192	781.347	1.120	0.045	-0.180
360.000	6.0746	738.392	1.070	0.045	-0.215
369.998	8.3796	736.960	1.080	0.045	-0.408
379.997	10.7245	735.418	1.100	0.045	-0.546
379.997	9.5841	695.625	1.100	0.045	-0.658
379.998	8.5722	642.930	1.080	0.045	-1.049

379.999	7.5622	547.085	1.060	0.045	-2.452
379.997	6.9374	438.569	1.070	0.045	0.926
384.997	7.4265	438.059	1.110	0.045	0.920
389.998	7.9152	437.569	1.070	0.045	0.927
394.999	8.4026	436.992	1.070	0.045	0.938
400.003	8.8885	436.386	1.080	0.045	0.950
400.004	6.9608	267.334	1.090	0.045	0.365
400.002	5.6009	182.965	1.090	0.052	-0.526
400.003	4.3799	127.287	1.110	0.059	-0.400
400.005	3.6635	100.392	1.110	0.066	-0.414
400.004	2.7004	69.001	1.120	0.088	-0.409
400.005	1.9310	46.915	1.060	0.116	-0.420

[a]Reported values are averages of replicate measurements at each (T, p) state point. [b]Standard uncertainty in temperature is 3 mK. [c]Standard uncertainty in pressure. [d]Relative combined, expanded (k = 2) state-point uncertainty in density. [e]Relative deviation from default mixing model calculated according to eq 3.

Table 7. Measured Temperature (T), Pressure (p), and Density (ρ) Data for the 0.33342/0.66658 Molar R-1234yf + R-152a Blend[a]

T[b] /K	p /MPa	ρ /kg·m^{-3}	$u(p)$[c] /kPa	100·($U(\rho)/\rho$)[d]	$\Delta\rho$ [e]
Vapor-phase					
283.160	0.0799	2.842	0.030	0.130	-0.004
283.162	0.1508	5.468	0.030	0.076	0.004
283.160	0.2202	8.144	0.030	0.060	0.007
283.158	0.2916	11.016	0.030	0.054	0.017
273.157	0.0502	1.839	0.030	0.191	-0.018
273.156	0.1054	3.929	0.030	0.096	0.005
273.158	0.1522	5.758	0.030	0.074	0.011
273.159	0.2041	7.854	0.030	0.062	0.020
263.161	0.0518	1.976	0.030	0.180	-0.032
263.157	0.0873	3.373	0.030	0.110	0.001
263.156	0.1116	4.346	0.030	0.091	0.012
263.156	0.1409	5.551	0.030	0.076	0.028
263.156	0.1735	6.922	0.030	0.067	0.045
253.157	0.0492	1.955	0.030	0.184	-0.023
253.158	0.0666	2.665	0.030	0.137	0.015
253.157	0.0830	3.345	0.030	0.112	0.030
253.154	0.0986	3.997	0.030	0.098	0.042
253.153	0.1133	4.624	0.030	0.087	0.055
Liquid-phase and supercritical states					
230.020	1.0472	1151.219	2.210	0.046	-0.424
230.018	1.0635	1151.257	2.380	0.047	-0.424
240.014	9.0008	1144.452	2.360	0.047	-0.421
240.014	8.9980	1144.443	2.220	0.046	-0.421
240.019	7.1446	1140.893	2.240	0.047	-0.421
240.015	5.3569	1137.377	2.170	0.046	-0.421
240.018	3.6626	1133.932	2.750	0.048	-0.422
240.019	2.0462	1130.559	2.210	0.046	-0.423
250.004	11.2695	1127.517	3.230	0.049	-0.420
250.009	8.2840	1121.352	2.670	0.047	-0.421
250.010	6.5975	1117.730	1.800	0.045	-0.421
250.012	5.0000	1114.194	2.120	0.046	-0.421
250.009	3.4707	1110.719	1.750	0.045	-0.422
250.011	1.3163	1105.619	1.830	0.045	-0.423
260.005	9.8232	1102.703	1.850	0.045	-0.418
260.010	8.5414	1099.732	2.370	0.046	-0.418
260.011	7.0096	1096.087	3.110	0.048	-0.419
260.011	4.1349	1088.930	1.830	0.045	-0.420
260.011	2.7945	1085.433	1.820	0.045	-0.421
260.015	1.5166	1081.989	1.930	0.045	-0.422
270.002	9.3860	1079.196	2.300	0.046	-0.417
270.006	8.1882	1076.067	1.990	0.045	-0.418
270.008	6.8225	1072.405	1.920	0.045	-0.418
270.005	4.2551	1065.195	1.960	0.045	-0.420
270.008	2.3102	1059.398	1.990	0.045	-0.422

270.008	1.3251	1056.344	1.960	0.045	-0.423
280.001	8.5258	1053.560	1.660	0.045	-0.416
280.004	7.7161	1051.142	2.120	0.045	-0.417
280.003	6.5057	1047.444	2.070	0.045	-0.418
280.003	4.2329	1040.153	1.820	0.045	-0.420
280.003	3.1662	1036.553	1.940	0.045	-0.422
280.003	1.2964	1029.934	2.390	0.046	-0.425
295.004	11.2715	1026.368	1.780	0.045	-0.408
295.008	9.3983	1020.051	1.690	0.045	-0.409
295.009	8.3177	1016.254	2.110	0.045	-0.410
295.007	6.2872	1008.742	1.670	0.045	-0.412
295.007	4.4148	1001.318	1.810	0.045	-0.415
295.007	1.8852	990.365	2.620	0.047	-0.420
309.999	10.6636	987.241	1.150	0.044	-0.399
310.005	8.9567	980.125	1.310	0.044	-0.400
310.003	7.2372	972.484	1.620	0.044	-0.402
310.007	5.6559	964.916	1.420	0.044	-0.404
310.000	3.5108	953.701	1.260	0.044	-0.407
310.003	1.8399	943.956	1.200	0.044	-0.411
329.995	11.8304	940.218	1.240	0.044	-0.380
329.997	9.0360	925.094	1.380	0.044	-0.381
329.996	7.1407	913.462	1.270	0.044	-0.382
329.995	4.9542	898.115	1.170	0.044	-0.384
329.997	3.5434	886.701	1.130	0.044	-0.387
329.996	1.9344	871.615	1.170	0.044	-0.396
340.006	5.8295	869.957	1.100	0.044	-0.371
349.998	9.7291	868.405	1.100	0.044	-0.360
350.002	7.8577	852.439	1.160	0.044	-0.358
349.998	5.9258	832.692	1.300	0.044	-0.356
349.999	4.3632	812.784	1.100	0.044	-0.357
349.997	2.9535	789.452	1.140	0.044	-0.365
370.005	8.8163	787.012	1.060	0.044	-0.338
370.001	6.9835	758.721	1.050	0.044	-0.323
370.005	5.8222	734.690	1.080	0.044	-0.303
385.001	9.4942	733.132	1.070	0.044	-0.335
385.003	6.7567	664.679	1.070	0.044	0.653
385.004	5.5541	600.643	1.050	0.044	-0.037
400.003	7.8504	599.561	1.050	0.044	0.297

[a]Reported values are averages of replicate measurements at each (T, p) state point. [b]Standard uncertainty in temperature is 3 mK. [c]Standard uncertainty in pressure. [d]Relative combined, expanded (k = 2) state-point uncertainty in density. [e]Relative deviation from default mixing model calculated according to eq 3.

Table 8. Measured Temperature (T), Pressure (p), and Density (ρ) Data for the 0.66526/0.33474 Molar R-1234yf + R-152a Blend[a]

T[b] /K	p /MPa	ρ /kg·m^{-3}	$u(p)$[c] /kPa	$100\cdot(U(\rho)/\rho)$[d]	$\Delta\rho$ [e]
Vapor-phase					
283.147	0.0816	3.468	0.030	0.117	-0.029
283.150	0.1526	6.611	0.030	0.071	-0.033
283.149	0.2244	9.921	0.030	0.057	-0.042
283.147	0.2916	13.161	0.030	0.051	-0.053
273.155	0.0516	2.259	0.030	0.168	-0.035
273.154	0.1027	4.566	0.030	0.091	-0.031
273.152	0.1528	6.901	0.030	0.069	-0.035
273.150	0.2052	9.430	0.030	0.058	-0.040
273.150	0.2511	11.727	0.030	0.053	-0.044
263.151	0.0603	2.752	0.030	0.144	-0.043
263.149	0.0926	4.278	0.030	0.101	-0.036
263.149	0.1217	5.682	0.030	0.082	-0.035
263.150	0.1541	7.280	0.030	0.067	-0.035
263.151	0.1826	8.722	0.030	0.061	-0.034
253.161	0.0521	2.471	0.030	0.161	-0.058
253.159	0.0751	3.596	0.030	0.120	-0.041
253.158	0.0894	4.309	0.030	0.100	-0.036
253.158	0.1030	4.994	0.030	0.087	-0.034
253.158	0.1159	5.651	0.030	0.080	-0.033
Liquid-phase and supercritical states					
230.012	3.5882	1238.587	2.330	0.047	-0.367
230.015	2.0030	1235.099	2.440	0.047	-0.367
230.014	1.2189	1233.345	3.130	0.050	-0.367
240.006	10.3783	1229.689	2.460	0.047	-0.369
240.011	8.6313	1225.870	2.320	0.046	-0.369
240.009	6.9432	1222.081	1.810	0.045	-0.369
240.010	3.8119	1214.735	2.140	0.046	-0.370
240.014	1.4066	1208.780	1.510	0.044	-0.370
250.015	9.8946	1205.282	2.170	0.046	-0.368
250.019	8.2884	1201.360	2.000	0.045	-0.368
250.019	6.7596	1197.516	2.010	0.045	-0.369
250.018	3.9092	1190.024	1.910	0.045	-0.369
250.023	1.4647	1183.199	1.750	0.045	-0.370
260.006	9.3265	1179.914	1.690	0.044	-0.369
260.009	7.9322	1176.078	1.780	0.045	-0.370
260.010	6.5802	1172.246	1.820	0.045	-0.371
260.010	5.2804	1168.449	1.810	0.045	-0.372
260.010	4.0380	1164.712	1.900	0.045	-0.372
270.007	7.7279	1150.383	1.740	0.044	-0.368
270.011	6.5213	1146.512	1.790	0.045	-0.369
280.003	7.8745	1124.997	1.600	0.044	-0.365
280.003	6.1600	1118.748	3.490	0.051	-0.367
280.004	3.8889	1109.926	1.910	0.045	-0.370
280.005	2.5799	1104.513	1.970	0.045	-0.372

280.003	1.3878	1099.354	1.560	0.044	-0.375
295.003	5.0318	1071.467	1.990	0.045	-0.359
295.003	3.4860	1063.701	1.540	0.044	-0.363
295.001	2.7610	1059.863	1.560	0.044	-0.366
295.002	1.4027	1052.268	1.390	0.044	-0.371
310.004	9.2677	1048.627	1.430	0.044	-0.336
309.999	7.7192	1040.526	1.180	0.043	-0.339
310.008	6.2943	1032.477	1.320	0.043	-0.343
310.007	4.9751	1024.512	1.410	0.044	-0.346
310.000	3.7546	1016.577	1.380	0.044	-0.351
310.008	2.6362	1008.688	1.320	0.043	-0.357
310.005	1.6135	1000.932	1.160	0.043	-0.364
329.992	10.5400	996.879	1.100	0.043	-0.310
330.001	8.7042	984.474	1.250	0.043	-0.313
329.998	7.0684	972.163	1.170	0.043	-0.318
329.998	5.1791	955.903	1.120	0.043	-0.329
329.998	3.5838	939.787	1.150	0.043	-0.345
330.001	1.9555	919.832	1.160	0.043	-0.379
339.999	5.3752	918.075	1.080	0.043	-0.323
349.999	8.8171	916.486	1.100	0.043	-0.300
350.003	7.6684	903.998	1.100	0.043	-0.303
350.002	5.7595	879.209	1.120	0.043	-0.315
350.002	4.2933	854.585	1.090	0.043	3.533
350.004	2.8974	821.915	1.060	0.043	3.740
360.003	5.3567	820.585	1.050	0.043	2.156
370.003	7.8529	819.304	1.050	0.043	1.756
370.009	7.0335	802.520	1.090	0.043	1.626
370.007	6.0414	777.444	1.090	0.043	1.413
370.009	5.0824	744.093	1.060	0.043	1.106
385.002	7.9903	742.552	1.050	0.049	1.095
385.008	6.8049	700.104	1.030	0.049	0.767
385.005	5.5527	618.173	1.050	0.049	0.266
390.002	6.1951	617.777	1.040	0.049	0.307
395.000	6.8439	617.376	1.040	0.049	0.347
400.003	7.4991	616.997	1.050	0.049	0.389
400.006	6.2695	505.542	1.060	0.049	0.134
400.008	5.5737	393.566	1.060	0.049	0.194
400.008	4.8936	282.970	1.070	0.049	-0.352
400.006	4.1641	201.445	1.090	0.054	-0.117
400.007	2.5249	94.225	1.100	0.083	-0.153
400.010	1.4067	46.536	1.110	0.148	-0.254

[a]Reported values are averages of replicate measurements at each (T, p) state point. [b]Standard uncertainty in temperature is 3 mK. [c]Standard uncertainty in pressure. [d]Relative combined, expanded (k = 2) state-point uncertainty in density. [e]Relative deviation from default mixing model calculated according to eq 3.

Table 9. Measured Temperature (T), Pressure (p), and Density (ρ) Data for the 0.33265/0.66735 Molar R-1234ze(E) + R-227ea Blend[a]

T[b] /K	p /MPa	ρ /kg·m^{-3}	$u(p)$[c] /kPa	$100\cdot(U(\rho)/\rho)$[d]	$\Delta\rho$ [e]
Vapor-phase					
293.149	0.1040	6.641	0.030	0.073	-0.144
293.148	0.1547	10.031	0.030	0.052	-0.093
293.149	0.2017	13.279	0.030	0.043	-0.069
293.152	0.2520	16.865	0.030	0.036	-0.054
293.152	0.3012	20.505	0.030	0.033	-0.045
283.151	0.0745	4.895	0.030	0.099	-0.096
283.153	0.1301	8.718	0.030	0.060	-0.047
283.152	0.1815	12.392	0.030	0.045	-0.029
283.152	0.2311	16.076	0.030	0.038	-0.018
273.150	0.0510	3.461	0.030	0.141	-0.086
273.147	0.0892	6.138	0.030	0.082	-0.041
273.146	0.1170	8.141	0.030	0.064	-0.025
273.146	0.1472	10.366	0.030	0.052	-0.014
263.152	0.0535	3.778	0.030	0.133	-0.071
263.150	0.0768	5.486	0.030	0.092	-0.040
263.150	0.0914	6.566	0.030	0.078	-0.028
263.150	0.1117	8.104	0.030	0.065	-0.015
Liquid-phase and supercritical states					
229.999	0.9861	1555.527	1.820	0.029	-0.244
230.000	0.9866	1555.528	1.580	0.028	-0.244
244.991	14.9409	1548.151	1.980	0.030	-0.235
244.990	14.9337	1548.136	1.570	0.027	-0.235
244.992	10.8100	1537.809	1.520	0.027	-0.237
244.994	8.8795	1532.725	1.730	0.028	-0.239
244.993	5.3052	1522.847	1.640	0.028	-0.243
244.996	3.6531	1518.036	1.470	0.027	-0.245
244.993	1.1368	1510.414	1.630	0.028	-0.248
259.988	13.9013	1504.539	1.730	0.028	-0.238
259.990	13.8643	1504.429	1.300	0.026	-0.238
259.991	10.3273	1493.983	1.660	0.027	-0.242
259.993	7.1155	1483.817	1.700	0.028	-0.247
259.992	4.2000	1473.948	1.650	0.028	-0.252
259.993	2.8495	1469.127	1.530	0.027	-0.255
259.994	1.5704	1464.399	1.680	0.028	-0.258
279.995	16.5333	1457.129	1.460	0.026	-0.246
279.995	10.5871	1436.086	1.550	0.027	-0.258
279.997	7.9789	1425.822	1.560	0.027	-0.265
279.996	4.4884	1410.821	1.530	0.026	-0.278
279.999	2.4119	1401.042	1.480	0.026	-0.287
279.996	1.4259	1396.146	1.370	0.026	-0.292
304.996	17.0931	1388.601	1.570	0.026	-0.271
305.000	15.8052	1383.090	1.860	0.028	-0.275
304.997	13.4182	1372.342	1.580	0.026	-0.284
304.997	10.2043	1356.488	1.400	0.026	-0.300

304.999	8.2742	1346.047	1.350	0.025	-0.311
304.996	5.6738	1330.620	1.570	0.027	-0.331
304.999	4.0881	1320.225	1.500	0.026	-0.346
304.996	1.3183	1299.773	1.270	0.025	-0.382
314.989	6.1497	1296.999	1.110	0.025	-0.358
324.989	10.9690	1294.439	1.160	0.025	-0.339
334.991	15.7613	1292.032	1.180	0.025	-0.323
334.994	15.7444	1291.919	1.280	0.025	-0.323
334.992	13.1650	1275.380	1.430	0.026	-0.342
334.992	10.2027	1253.707	1.250	0.025	-0.372
334.992	8.2877	1237.653	1.190	0.025	-0.398
334.992	6.0941	1216.515	1.160	0.025	-0.438
334.991	3.8514	1190.404	1.160	0.025	-0.500
334.991	1.7759	1159.448	1.090	0.025	-0.599
344.988	5.0415	1157.442	1.070	0.025	-0.527
354.990	8.3267	1155.499	1.060	0.025	-0.479
364.994	11.6163	1153.606	1.100	0.025	-0.443
369.993	13.2460	1152.542	1.120	0.025	-0.428
369.994	11.7835	1135.768	1.180	0.025	-0.457
369.995	10.0904	1113.522	1.120	0.025	-0.501
369.995	8.0270	1080.384	1.130	0.025	-0.580
369.995	6.4395	1047.470	1.090	0.025	-0.680
369.997	5.0717	1009.361	1.080	0.025	-0.835
374.993	6.1473	1008.445	1.050	0.025	-0.780
379.991	7.2328	1007.651	1.050	0.025	-0.733
384.992	8.3237	1006.854	1.050	0.025	-0.694
389.993	9.4166	1006.041	1.080	0.026	-0.658
394.992	10.5107	1005.211	1.070	0.026	-0.627
399.995	11.6055	1004.359	1.080	0.026	-0.599
399.997	9.9974	967.751	1.120	0.026	-0.695
399.996	8.7299	930.761	1.090	0.026	-0.811
399.996	7.7584	894.130	1.060	0.026	-0.952
399.998	5.9793	783.461	1.060	0.026	2.320
399.997	4.9815	637.185	1.070	0.026	1.696
399.997	4.4682	492.634	1.090	0.026	1.163
399.997	3.7686	314.324	1.110	0.040	-1.704
399.994	1.8695	104.334	1.160	0.104	-0.351

[a]Reported values are averages of replicate measurements at each (T, p) state point. [b]Standard uncertainty in temperature is 3 mK. [c]Standard uncertainty in pressure. [d]Relative combined, expanded (k = 2) state-point uncertainty in density. [e]Relative deviation from default mixing model calculated according to eq 3.

Table 10. Measured Temperature (T), Pressure (p), and Density (ρ) Data for the 0.66803/0.33197 Molar R-1234ze(E) + R-227ea Blend[a]

T[b] /K	p /MPa	ρ /kg·m^{-3}	$u(p)$[c] /kPa	100·($U(\rho)/\rho$)[d]	$\Delta\rho$ [e]
Vapor-phase					
293.153	0.1027	5.743	0.030	0.101	0.008
293.155	0.1525	8.644	0.030	0.058	0.012
293.155	0.2011	11.568	0.030	0.063	0.013
293.154	0.2511	14.665	0.030	0.038	0.013
293.152	0.3011	17.872	0.030	0.034	0.015
283.153	0.0988	5.730	0.030	0.077	0.011
283.150	0.1461	8.608	0.030	0.055	0.018
283.150	0.1862	11.119	0.030	0.045	0.024
283.150	0.2203	13.316	0.030	0.040	0.030
283.151	0.2403	14.627	0.030	0.038	0.036
273.153	0.0786	4.716	0.030	0.096	0.008
273.151	0.1037	6.274	0.030	0.073	0.017
273.151	0.1267	7.732	0.030	0.061	0.026
273.152	0.1545	9.532	0.030	0.052	0.038
263.154	0.0495	3.055	0.030	0.149	-0.010
263.150	0.0756	4.721	0.030	0.097	0.015
263.150	0.1072	6.779	0.030	0.072	0.041
263.149	0.0490	3.028	0.030	0.150	-0.014
263.148	0.0750	4.683	0.030	0.098	0.014
263.148	0.1065	6.733	0.030	0.070	0.039
Liquid-phase and supercritical states					
230.021	0.8724	1463.129	1.480	0.027	-0.294
230.022	0.8715	1463.124	1.480	0.027	-0.294
245.014	14.5143	1454.515	1.750	0.028	-0.282
245.016	14.4826	1454.438	1.540	0.027	-0.282
245.019	12.3667	1449.668	2.320	0.031	-0.283
245.017	9.0813	1441.954	1.820	0.029	-0.285
245.021	6.5602	1435.729	1.880	0.029	-0.288
245.018	4.1116	1429.441	1.590	0.027	-0.290
245.021	1.5969	1422.656	1.500	0.027	-0.294
260.022	14.8871	1417.173	1.910	0.029	-0.281
260.026	12.1506	1410.033	1.830	0.028	-0.284
260.023	8.9920	1401.356	1.670	0.028	-0.289
260.027	6.5178	1394.151	1.680	0.027	-0.294
260.023	4.0205	1386.507	1.670	0.027	-0.299
260.028	1.6441	1378.786	1.370	0.026	-0.306
280.012	17.3175	1372.264	1.650	0.027	-0.291
280.011	15.0199	1365.316	1.600	0.027	-0.296
280.014	12.0422	1355.786	1.760	0.027	-0.303
280.012	9.0096	1345.387	1.430	0.026	-0.313
280.015	6.6239	1336.613	1.650	0.027	-0.322
280.011	3.4368	1323.938	1.620	0.027	-0.337
280.013	1.3175	1314.750	1.410	0.026	-0.350
305.004	17.6944	1307.692	1.340	0.025	-0.318

305.007	16.3395	1302.510	1.650	0.026	-0.323
305.004	12.6543	1287.425	1.370	0.026	-0.341
305.009	10.4406	1277.495	1.370	0.025	-0.354
305.005	8.4017	1267.691	1.340	0.025	-0.369
305.005	5.8321	1254.172	1.280	0.025	-0.393
305.007	4.0855	1244.072	1.180	0.025	-0.414
305.004	1.6357	1228.349	1.510	0.026	-0.452
314.999	6.7679	1225.690	1.360	0.025	-0.418
324.995	11.8094	1222.849	1.240	0.025	-0.391
334.996	16.7683	1219.956	1.200	0.025	-0.367
334.999	15.7836	1214.621	1.510	0.026	-0.375
334.997	13.1002	1198.997	1.420	0.026	-0.400
334.998	10.0133	1178.485	1.360	0.026	-0.439
334.998	8.0214	1163.307	1.240	0.025	-0.473
334.997	6.2764	1148.313	1.160	0.025	-0.511
334.997	3.8496	1123.670	1.230	0.025	-0.589
334.997	1.9336	1099.329	1.120	0.025	-0.692
344.994	5.4581	1097.384	1.100	0.025	-0.598
354.996	8.9976	1095.521	1.090	0.025	-0.537
365.001	12.5344	1093.686	1.140	0.025	-0.492
370.001	14.2800	1092.621	1.140	0.025	-0.474
370.004	12.1612	1071.507	1.190	0.025	-0.520
370.002	9.9662	1045.478	1.180	0.025	-0.587
370.003	7.8835	1014.625	1.130	0.025	-0.682
370.003	6.5252	989.155	1.090	0.025	-0.780
370.002	5.0868	953.779	1.090	0.026	-0.958
375.000	6.2390	953.042	1.050	0.025	-0.892
380.000	7.3978	952.287	1.050	0.025	-0.838
384.999	8.5599	951.516	1.060	0.026	-0.791
389.999	9.7248	950.730	1.060	0.026	-0.750
394.999	10.8905	949.925	1.080	0.026	-0.713
400.001	12.0560	949.099	1.070	0.026	-0.678
400.006	10.3536	914.763	1.100	0.026	-0.791
400.005	9.0348	880.665	1.090	0.026	-0.927
400.005	7.2391	812.957	1.060	0.026	-1.291
400.005	6.1877	745.823	1.050	0.027	-1.838
400.006	5.1617	608.454	1.060	0.027	2.042
400.005	4.5560	436.924	1.080	0.027	1.311
400.006	3.8005	268.422	1.110	0.041	-1.707
400.006	2.0830	103.749	1.140	0.091	-0.421
400.007	1.5420	71.612	1.150	0.131	-0.380

[a]Reported values are averages of replicate measurements at each (T, p) state point. [b]Standard uncertainty in temperature is 3 mK. [c]Standard uncertainty in pressure. [d]Relative combined, expanded (k = 2) state-point uncertainty in density. [e]Relative deviation from default mixing model calculated according to eq 3.

Table 11. Relative Deviations of Experimental Data from Values Calculated with Default Mixture Models

Data Source	AAD[a]	MAD[b]
R-32 + R-1234yf		
this work	0.368	2.606
Cai et al.[54]	0.238	0.659
Dang et al.[55]	0.624	1.657
Jia et al.[56]	0.258	0.971
Kobayashi et al.[50]	3.750	43.402
Tomassetti et al.[57]	0.350	4.538
Yang et al.[58]	0.228	0.628
R-32 + R-1234ze(E)		
this work	0.445	2.452
Jia et al.[59]	0.507	1.668
Kobayashi et al.[51]	3.674	16.701
Tanaka et al.[60]	0.227	0.436
Tomassetti et al.[61]	0.264	5.313
Yamaya et al.[62]	0.713	1.070
R-1234yf + R-152a		
this work	0.377	3.740
Tomassetti[52]	0.166	0.777
R-1234ze(E) + R-227ea		
this work	0.410	2.320

[a]Average absolute deviation calculated according to eq 6. [b]Maximum absolute deviation calculated according to eq 7.

Table 12. Relative Deviations of Experimental Data from Values Calculated with Updated Mixture Models[27, 28, 53]

Refrigerant Blend	AAD[a]	MAD[b]
R-32 + R-1234yf	0.120	4.158
R-32 + R-1234ze(E)	0.060	0.617
R-1234yf + R-152a	0.034	0.551
R-1234ze(E) + R-227ea	0.029	0.373

[a]Average absolute deviation calculated according to eq 6. [b]Maximum absolute deviation calculated according to eq 7.

Figure Captions

Figure 1. Molecular representations of refrigerants used in the binary mixtures studied in this work: R-32, R-152a, R-227ea, R-1234yf, and R-1234ze(E). Carbon atoms are black, hydrogen atoms are grey, and fluorine atoms are blue. Diagrams were constructed using Avogadro.[63]

Figure 2. Measured (p, ρ, T, x) state points for blends containing R-1234yf plotted as density vs temperature. On top are data for two compositions of R-32 + R-1234yf with x_1 = 0.33681 molar shown in (a) and x_1 = 0.67205 molar shown in (b). On bottom are data for two compositions of R-1234yf + R-152a with x_1 = 0.33342 molar shown in (c) and x_1 = 0.66526 molar shown in (d). For all graphs: ○, measured points; —, phase boundary; ✳, critical point. The phase boundaries and critical points were calculated using the default mixture models included in REFPROP (Version 10.0).[30]

Figure 3. Measured (p, ρ, T, x) state points for blends containing R-1234ze(E) plotted as density vs temperature. On top are data for two compositions of R-32 + R-1234ze(E) with x_1 = 0.33512 molar shown in (a) and x_1 = 0.66665 molar shown in (b). On bottom are data for two compositions of R-1234ze(E) + R-227ea with x_1 = 0.33265 molar shown in (c) and x_1 = 0.66803 molar shown in (d). For all graphs: ○, measured points; —, phase boundary; ✳, critical point. The phase boundaries and critical points were calculated using the default mixture models included in REFPROP (Version 10.0).[30]

Figure 4. Relative deviations of the experimental (p, ρ, T, x) data for R-32 + R-1234yf from values calculated with REFPROP[30] plotted as a function of (a) temperature, (b) pressure, and (c) density. For all graphs, ○ represent data for the x_1 = 0.33681 molar blend, while □ represent data for the x_1 = 0.67205 molar blend. Additionally, black symbols represent vapor-phase data, red

symbols represent liquid-phase data, and blue symbols represent data above the critical temperature (T_c) with T_c = 359.842 K for the x_1 = 0.33681 molar blend and T_c = 352.635 K for the x_1 = 0.67205 molar blend. Dashed lines are smoothed representations of the overall combined, expanded uncertainty for this binary mixture. Insets show vapor-phase data in greater detail.

Figure 5. Relative deviations of the experimental (p, ρ, T, x) data for R-32 + R-1234ze(E) from values calculated with REFPROP[30] plotted as a function of (a) temperature, (b) pressure, and (c) density. For all graphs, ○ represent data for the x_1 = 0.33512 molar blend, while □ represent data for the x_1 = 0.66665 molar blend. Additionally, black symbols represent vapor-phase data, red symbols represent liquid-phase data, and blue symbols represent data above the critical temperature (T_c) with T_c = 377.566 K for the x_1 = 0.33512 molar blend and T_c = 366.416 K for the x_1 = 0.66665 molar blend. Dashed lines are smoothed representations of the overall combined, expanded uncertainty for this binary mixture. Insets show vapor-phase data in greater detail.

Figure 6. Relative deviations of the experimental (p, ρ, T, x) data for R-1234yf + R-152a from values calculated with REFPROP[30] plotted as a function of (a) temperature, (b) pressure, and (c) density. For all graphs, ○ represent data for the x_1 = 0.33342 molar blend, while □ represent data for the x_1 = 0.66526 molar blend. Additionally, black symbols represent vapor-phase data, red symbols represent liquid-phase data, and blue symbols represent data above the critical temperature (T_c) with T_c = 376.864 K for the x_1 = 0.33342 molar blend and T_c = 371.043 K for the x_1 = 0.66526 molar blend. Dashed lines are smoothed representations of the overall combined, expanded uncertainty for this binary mixture. Insets show vapor-phase data in greater detail.

Figure 7. Relative deviations of the experimental (p, ρ, T, x) data for R-1234ze(E) + R-227ea from values calculated with REFPROP[30] plotted as a function of (a) temperature, (b) pressure, and (c) density. For all graphs, ○ represent data for the x_1 = 0.33265 molar blend, while □ represent

data for the x_1 = 0.66803 molar blend. Additionally, black symbols represent vapor-phase data, red symbols represent liquid-phase data, and blue symbols represent data above the critical temperature (T_c) with T_c = 377.260 K for the x_1 = 0.33265 molar blend and T_c = 379.890 K for the x_1 = 0.66803 molar blend. Dashed lines are smoothed representations of the overall combined, expanded uncertainty for this binary mixture. Insets show vapor-phase data in greater detail.

Figure 8. Relative deviations of experimental density data from values calculated with REFPROP[30] plotted as a function of temperature for (a) R-32 + R-1234yf, (b) R-32 + R-1234ze(E), and (c) R-1234yf + R-152a. For R-32 + R-1234yf: ○, this work (x_1 = 0.33681 molar); □, this work (x_1 = 0.67205 molar); △, Cai et al.[54]; ⋈, Dang et al.[55]; ▽, Jia et al.[56]; ✳, Kobayashi et al.[50]; ⧖, Tomassetti et al.[57]; and +, Yang et al.[58]. For R-32 + R-1234ze(E): ○, this work (x_1 = 0.33512 molar); □, this work (x_1 = 0.66665 molar); △, Jia et al.[59]; ▽, Kobayashi et al.[51]; ⋈, Tanaka et al.[60]; ✳, Tomassetti et al.[61]; and +, Yamaya et al.[62]. For R-1234yf + R-152a: ○, this work (x_1 = 0.33342 molar); □, this work (x_1 = 0.66526 molar); and △, Tomassetti[52]. Additionally, the light orange shaded region designates the range of corresponding critical temperatures. Where needed, the graph region covering the majority of data points has been expanded and is shown in the inset for clarity.

Figure 9. Relative deviations of experimental density data from values calculated with REFPROP[30] plotted as a function of composition for (a) R-32 + R-1234yf, (b) R-32 + R-1234ze(E), and (c) R-1234yf + R-152a. For R-32 + R-1234yf: ○, this work (x_1 = 0.33681 molar); □, this work (x_1 = 0.67205 molar); △, Cai et al.[54]; ⋈, Dang et al.[55]; ▽, Jia et al.[56]; ✳, Kobayashi et al.[50]; ⧖, Tomassetti et al.[57]; and +, Yang et al.[58]. For R-32 + R-1234ze(E): ○, this work (x_1 = 0.33512 molar); □, this work (x_1 = 0.66665 molar); △, Jia et al.[59]; ▽, Kobayashi et al.[51]; ⋈, Tanaka et al.[60]; ✳, Tomassetti et al.[61]; and +, Yamaya et al.[62]. For R-1234yf + R-152a:

○, this work (x_1 = 0.33342 molar); □, this work (x_1 = 0.66526 molar); and △, Tomassetti[52]. Where needed, the graph region covering the majority of data points has been expanded and is shown in the inset for clarity.

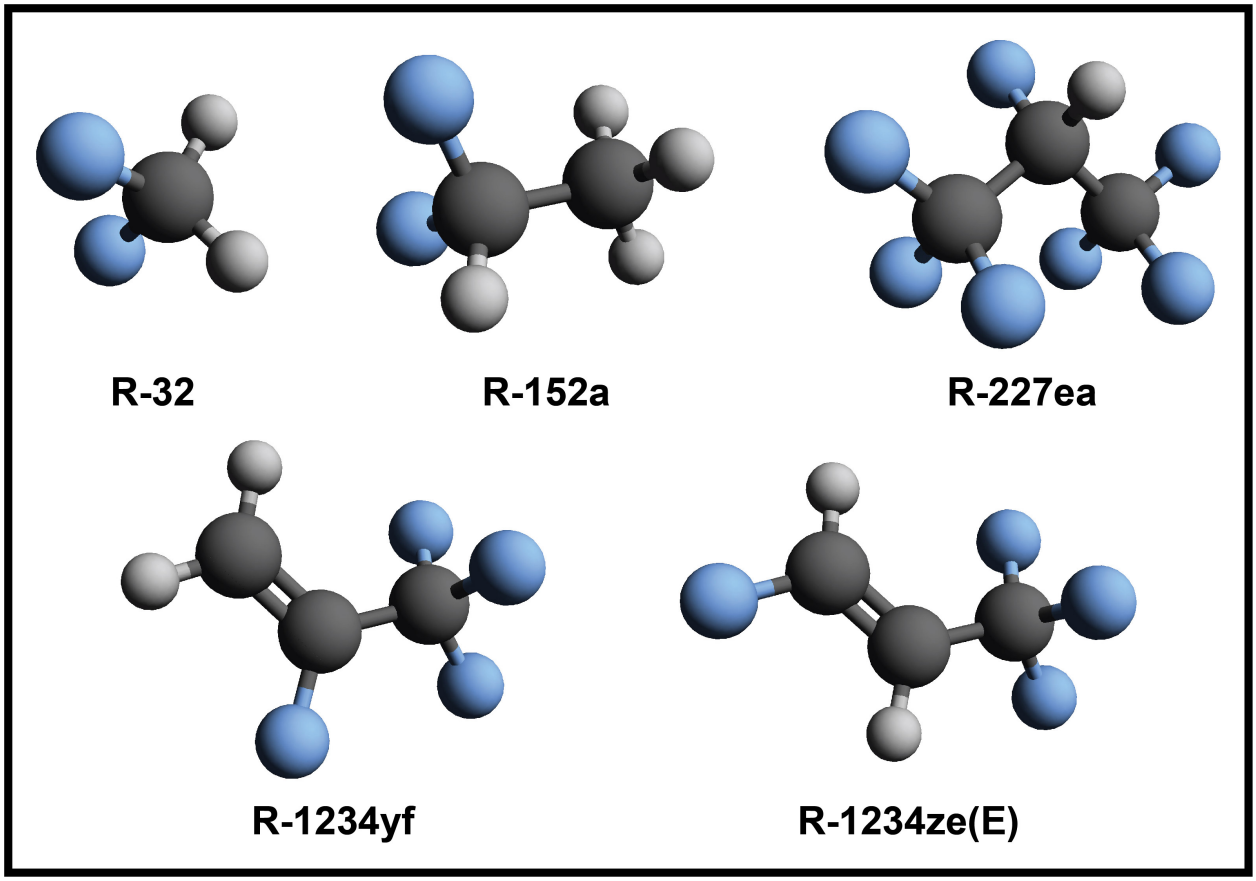

Figure 1. Molecular representations of refrigerants used in the binary mixtures studied in this work: R-32, R-152a, R-227ea, R-1234yf, and R-1234ze(E). Carbon atoms are black, hydrogen atoms are grey, and fluorine atoms are blue. Diagrams were constructed using Avogadro.[63]

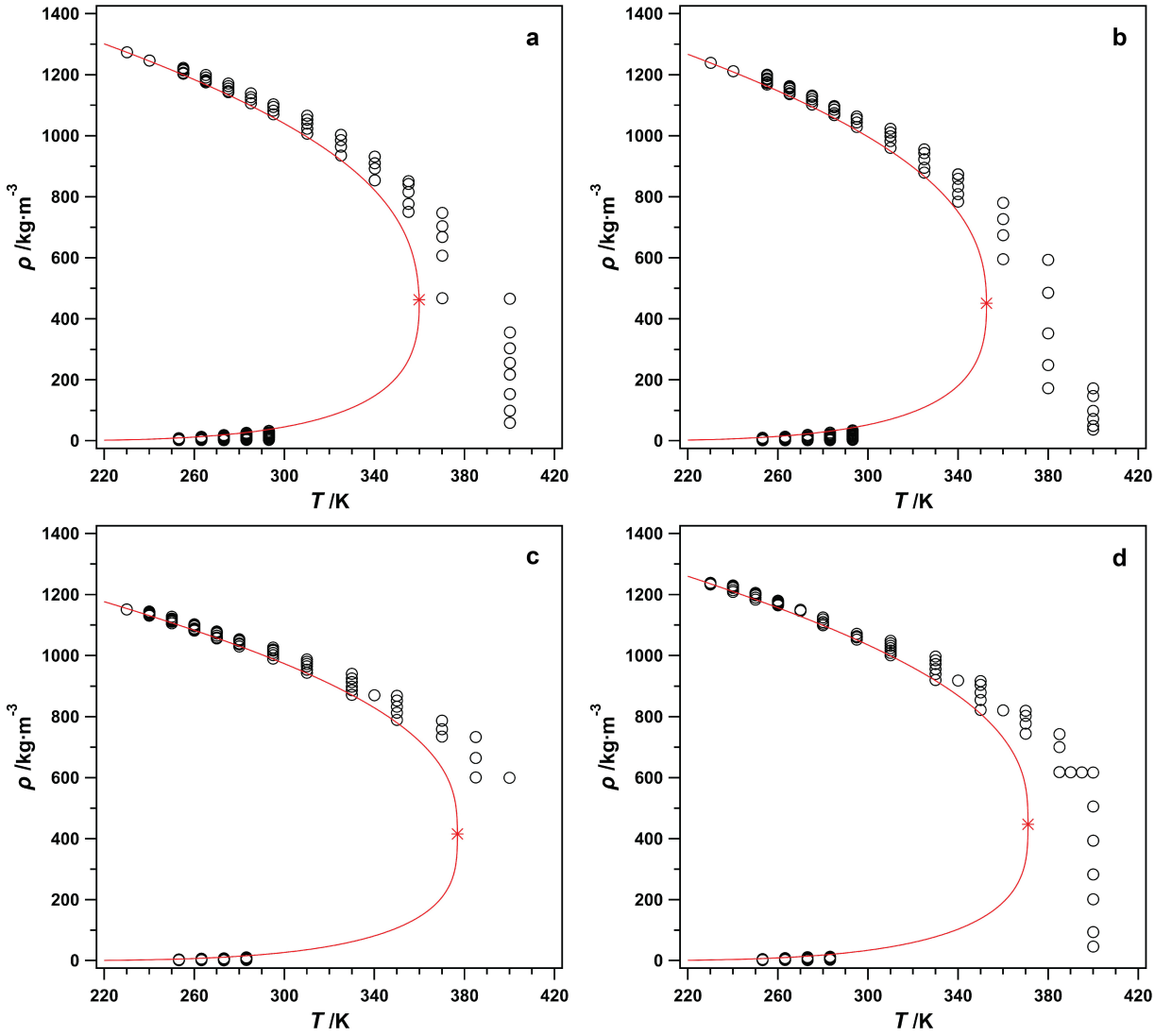

Figure 2. Measured (p, ρ, T, x) state points for blends containing R-1234yf plotted as density vs temperature. On top are data for two compositions of R-32 + R-1234yf with x_1 = 0.33681 molar shown in (a) and x_1 = 0.67205 molar shown in (b). On bottom are data for two compositions of R-1234yf + R-152a with x_1 = 0.33342 molar shown in (c) and x_1 = 0.66526 molar shown in (d). For all graphs: ○, measured points; —, phase boundary; ✳, critical point. The phase boundaries and critical points were calculated using the default mixture models included in REFPROP (Version 10.0).[30]

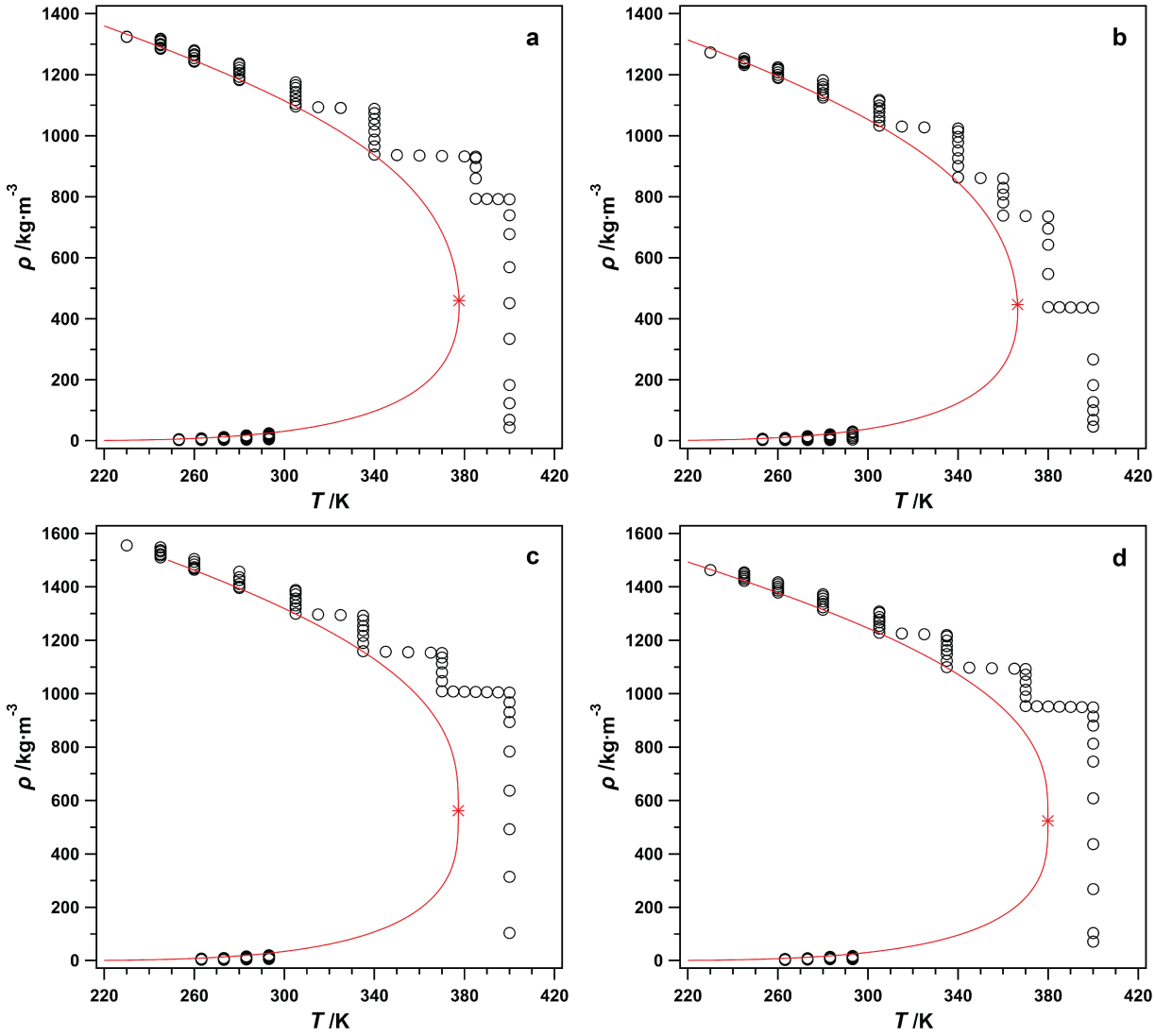

Figure 3. Measured (p, ρ, T, x) state points for blends containing R-1234ze(E) plotted as density vs temperature. On top are data for two compositions of R-32 + R-1234ze(E) with x_1 = 0.33512 molar shown in (a) and x_1 = 0.66665 molar shown in (b). On bottom are data for two compositions of R-1234ze(E) + R-227ea with x_1 = 0.33265 molar shown in (c) and x_1 = 0.66803 molar shown in (d). For all graphs: ○, measured points; —, phase boundary; ✳, critical point. The phase boundaries and critical points were calculated using the default mixture models included in REFPROP (Version 10.0).[30]

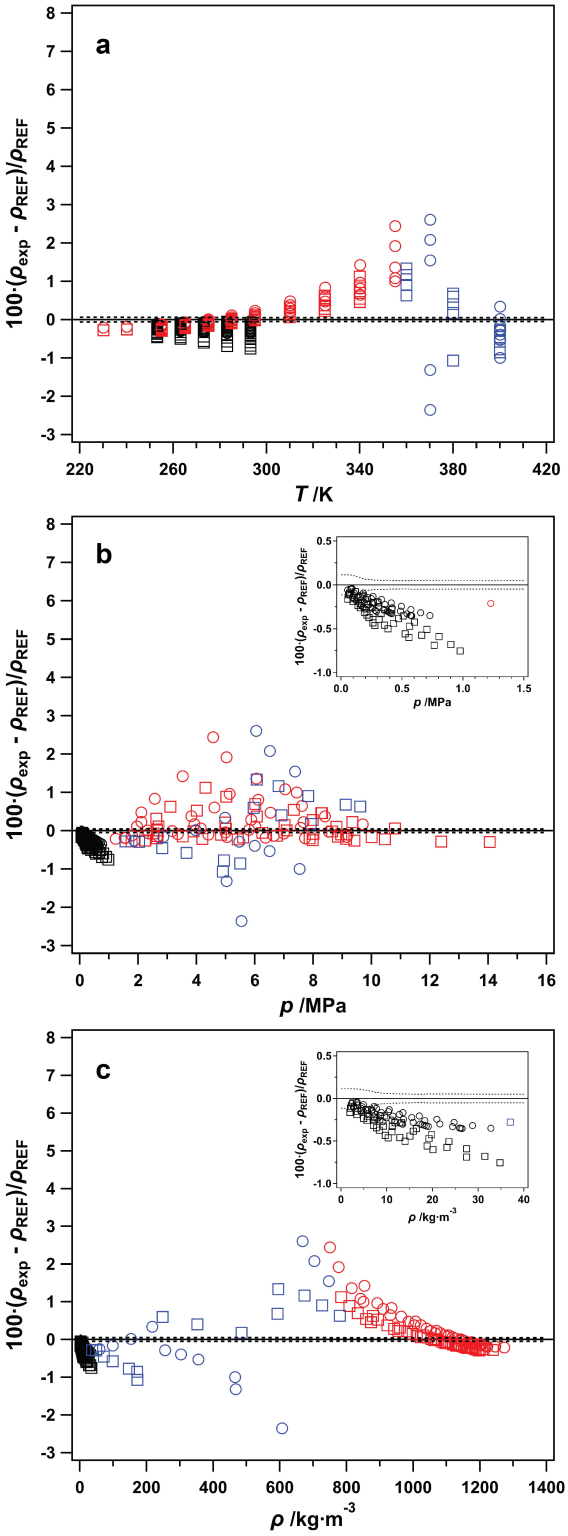

Figure 4. Relative deviations of the experimental (p, ρ, T, x) data for R-32 + R-1234yf from values calculated with REFPROP[30] plotted as a function of (a) temperature, (b) pressure, and (c) density. For all graphs, ○ represent data for the x_1 = 0.33681 molar blend, while □ represent data for the x_1 = 0.67205 molar blend. Additionally, black symbols represent vapor-phase data,

red symbols represent liquid-phase data, and blue symbols represent data above the critical temperature (T_c) with T_c = 359.842 K for the x_1 = 0.33681 molar blend and T_c = 352.635 K for the x_1 = 0.67205 molar blend. Dashed lines are smoothed representations of the overall combined, expanded uncertainty for this binary mixture. Insets show vapor-phase data in greater detail.

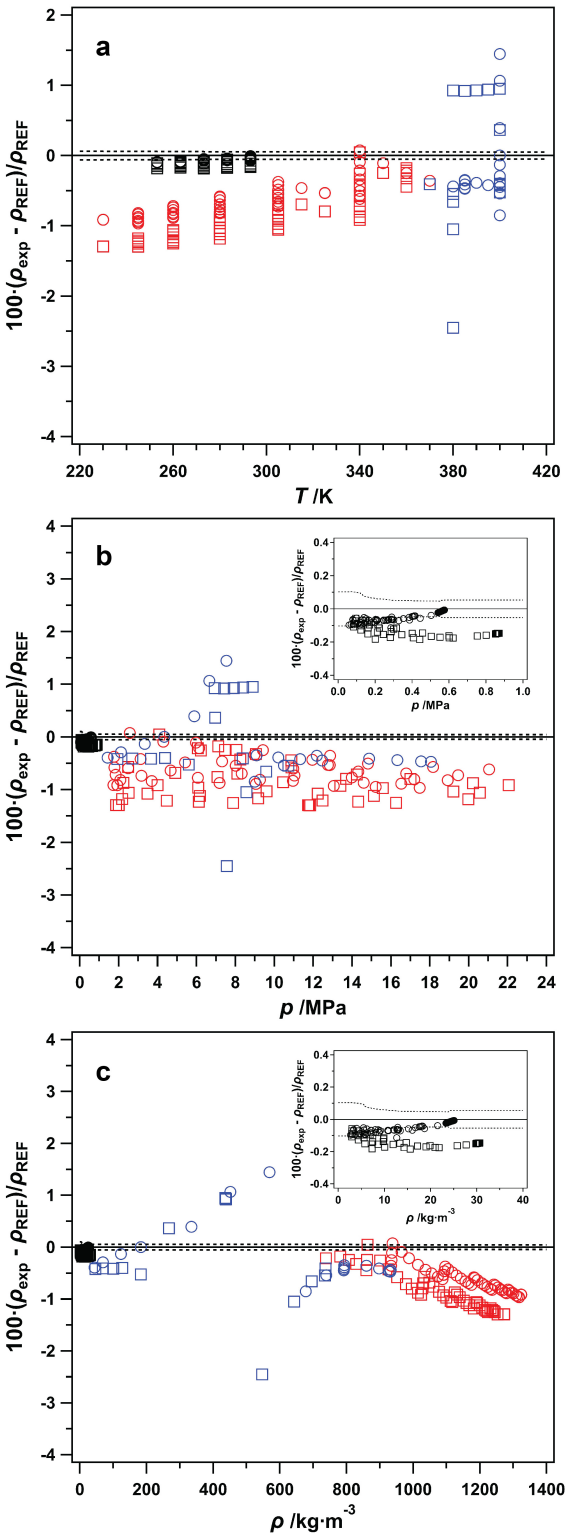

Figure 5. Relative deviations of the experimental (p, ρ, T, x) data for R-32 + R-1234ze(E) from values calculated with REFPROP[30] plotted as a function of (a) temperature, (b) pressure, and (c) density. For all graphs, ○ represent data for the $x_1 = 0.33512$ molar blend, while □ represent data for the $x_1 = 0.66665$ molar blend. Additionally, black symbols represent vapor-phase data,

red symbols represent liquid-phase data, and blue symbols represent data above the critical temperature (T_c) with T_c = 377.566 K for the x_1 = 0.33512 molar blend and T_c = 366.416 K for the x_1 = 0.66665 molar blend. Dashed lines are smoothed representations of the overall combined, expanded uncertainty for this binary mixture. Insets show vapor-phase data in greater detail.

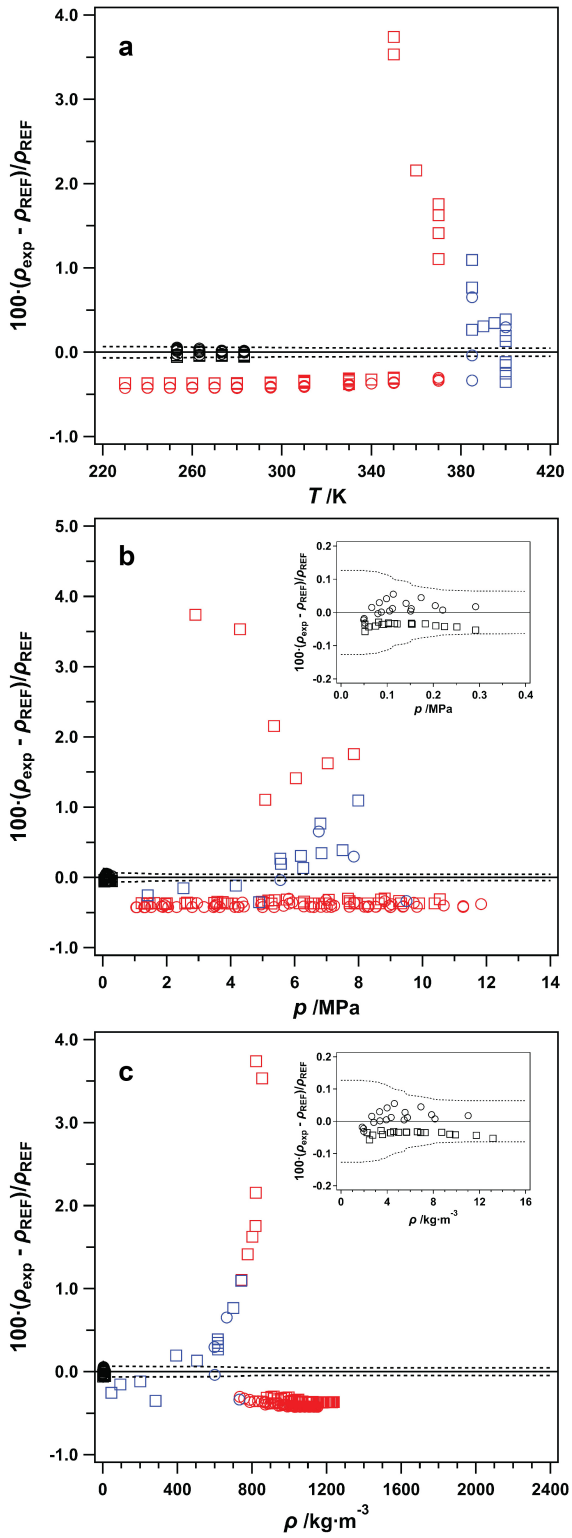

Figure 6. Relative deviations of the experimental (p, ρ, T, x) data for R-1234yf + R-152a from values calculated with REFPROP[30] plotted as a function of (a) temperature, (b) pressure, and (c) density. For all graphs, ○ represent data for the $x_1 = 0.33342$ molar blend, while □ represent data for the $x_1 = 0.66526$ molar blend. Additionally, black symbols represent vapor-phase data,

red symbols represent liquid-phase data, and blue symbols represent data above the critical temperature (T_c) with T_c = 376.864 K for the x_1 = 0.33342 molar blend and T_c = 371.043 K for the x_1 = 0.66526 molar blend. Dashed lines are smoothed representations of the overall combined, expanded uncertainty for this binary mixture. Insets show vapor-phase data in greater detail.

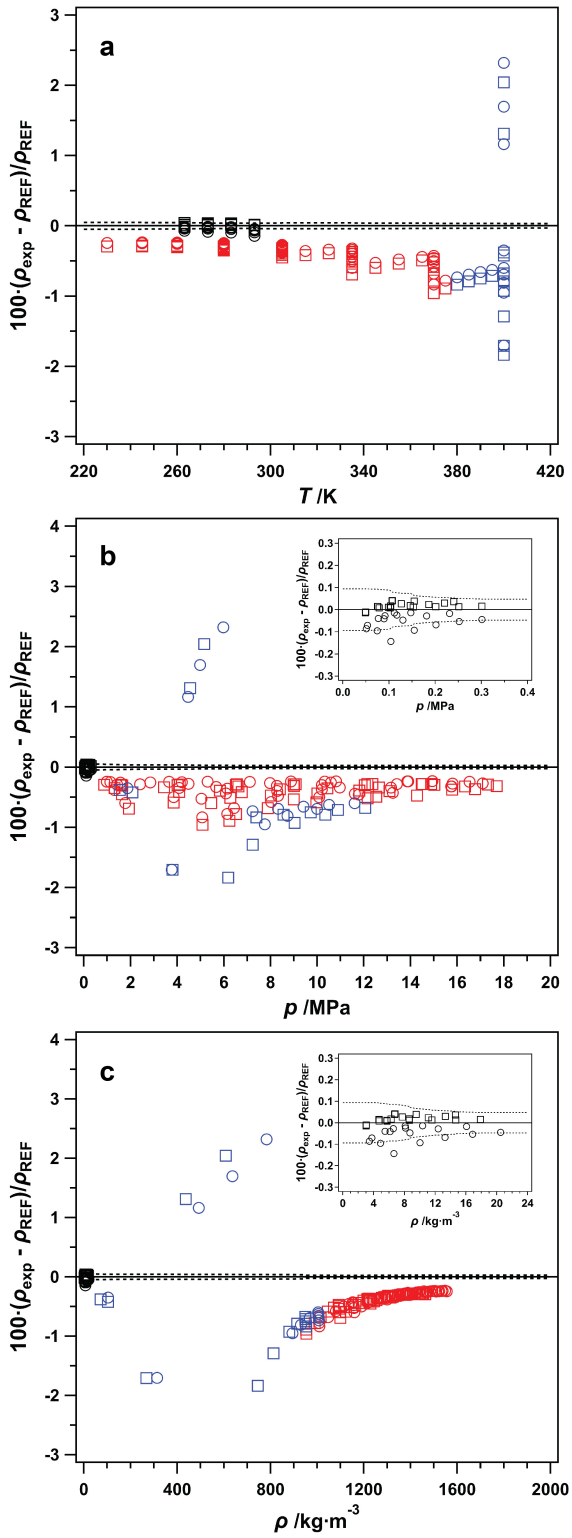

Figure 7. Relative deviations of the experimental (p, ρ, T, x) data for R-1234ze(E) + R-227ea from values calculated with REFPROP[30] plotted as a function of (a) temperature, (b) pressure, and (c) density. For all graphs, ○ represent data for the $x_1 = 0.33265$ molar blend, while □ represent data for the $x_1 = 0.66803$ molar blend. Additionally, black symbols represent vapor-

phase data, red symbols represent liquid-phase data, and blue symbols represent data above the critical temperature (T_c) with T_c = 377.260 K for the x_1 = 0.33265 molar blend and T_c = 379.890 K for the x_1 = 0.66803 molar blend. Dashed lines are smoothed representations of the overall combined, expanded uncertainty for this binary mixture. Insets show vapor-phase data in greater detail.

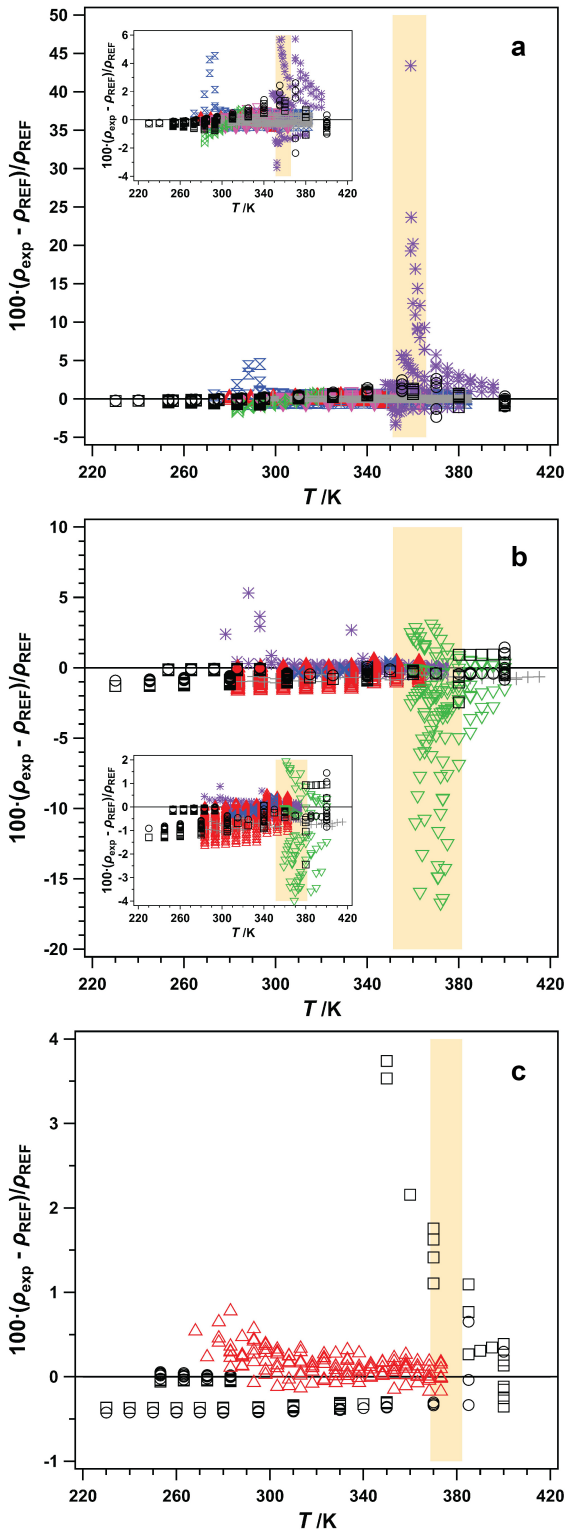

Figure 8. Relative deviations of experimental density data from values calculated with REFPROP[30] plotted as a function of temperature for (a) R-32 + R-1234yf, (b) R-32 + R-1234ze(E), and (c) R-1234yf + R-152a. For R-32 + R-1234yf: ○, this work (x_1 = 0.33681 molar); □, this work (x_1 = 0.67205 molar); △, Cai et al.[54]; ⋈, Dang et al.[55]; ▽, Jia et al.[56]; ✳,

Kobayashi et al.[50]; ⧖, Tomassetti et al.[57]; and +, Yang et al.[58]. For R-32 + R-1234ze(E): ○, this work (x_1 = 0.33512 molar); □, this work (x_1 = 0.66665 molar); △, Jia et al.[59]; ▽, Kobayashi et al.[51]; ⋈, Tanaka et al.[60]; ✳, Tomassetti et al.[61]; and +, Yamaya et al.[62]. For R-1234yf + R-152a: ○, this work (x_1 = 0.33342 molar); □, this work (x_1 = 0.66526 molar); and △, Tomassetti[52]. Additionally, the light orange shaded region designates the range of corresponding critical temperatures. Where needed, the graph region covering the majority of data points has been expanded and is shown in the inset for clarity.

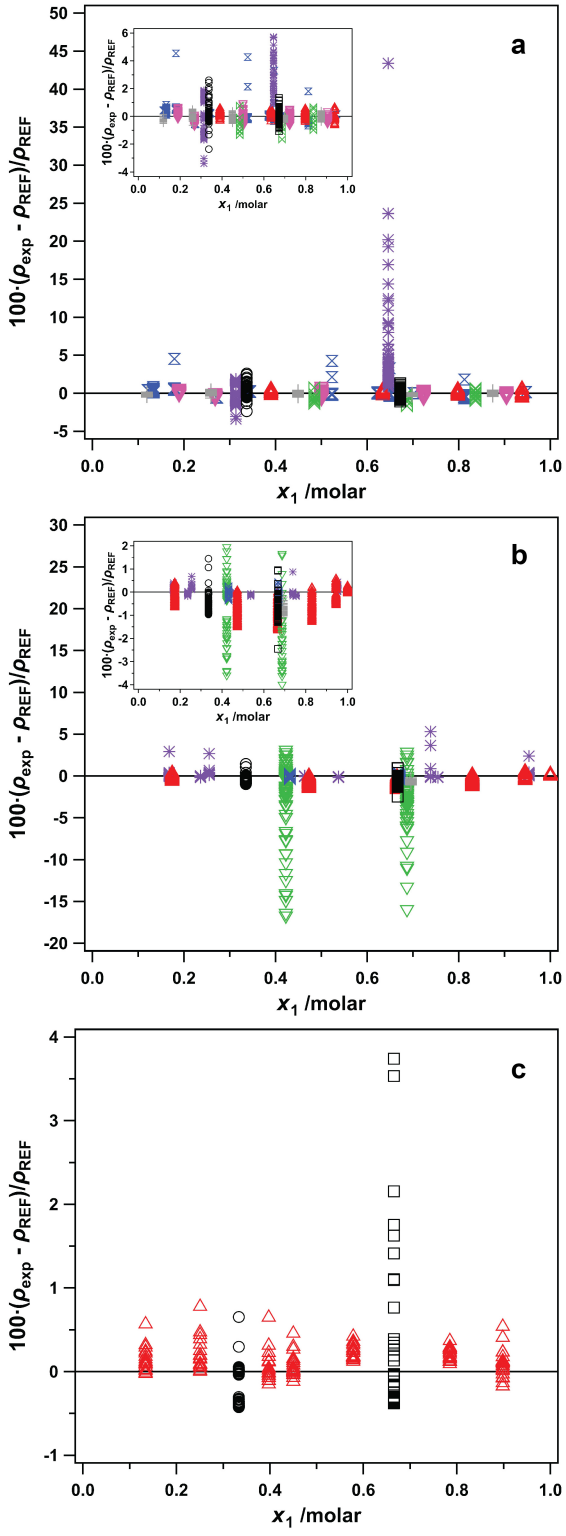

Figure 9. Relative deviations of experimental density data from values calculated with REFPROP[30] plotted as a function of composition for (a) R-32 + R-1234yf, (b) R-32 + R-1234ze(E), and (c) R-1234yf + R-152a. For R-32 + R-1234yf: ○, this work (x_1 = 0.33681 molar); □, this work (x_1 = 0.67205 molar); △, Cai et al.[54]; ⋈, Dang et al.[55]; ▽, Jia et al.[56]; ✳,

Kobayashi et al.[50]; ⧖, Tomassetti et al.[57]; and +, Yang et al.[58]. For R-32 + R-1234ze(E): ○, this work (x_1 = 0.33512 molar); □, this work (x_1 = 0.66665 molar); △, Jia et al.[59]; ▽, Kobayashi et al.[51]; ⋈, Tanaka et al.[60]; ✳, Tomassetti et al.[61]; and +, Yamaya et al.[62]. For R-1234yf + R-152a: ○, this work (x_1 = 0.33342 molar); □, this work (x_1 = 0.66526 molar); and △, Tomassetti[52]. Where needed, the graph region covering the majority of data points has been expanded and is shown in the inset for clarity.